

# Half-metallic ferromagnets

V Yu Irkhin, M I Katsnel'son

## Contents

1. Introduction	659
2. Band structure and magneto-optic properties	660
3. Transport properties and the problem of spin polarisation	664
4. Magnetic properties	665
5. Theoretical investigation of the energy spectrum within the framework of the s–d exchange and the Hubbard models: nonquasiparticle states	666
6. Nonquasiparticle contributions to electronic specific heat and transport properties	669
7. Ferromagnetism of systems with strong correlations	671
8. Microscopic model of transition-metal magnetism: analogies with half-metallic ferromagnets	673
9. Half-metallic antiferromagnets	674
10. Conclusions	675
References	675

**Abstract.** The experimental results, band structure calculations, and theoretical investigations carried out within the framework of the many-electron models of half-metallic ferromagnets (HMFs) are reviewed. These materials have an energy gap for one of the spin projections at the Fermi level and represent a separate class of strong itinerant magnetic substances, which includes some of the Heusler alloys (for example, PtMnSb), CrO<sub>2</sub>, etc. Some HMFs and related systems are promising magnetic materials which have, in particular, unique magneto-optic properties. The theoretical interest in HMFs arises from a striking manifestation of nonquasiparticle (spin-polaron) effects; for example, in the spin polarisation of charge carriers and in the nuclear magnetic relaxation rate. Concepts developed in the theory of HMFs are shown to be applicable also to ‘conventional’ strong itinerant (band) magnetic materials, including the iron-group metals.

## 1. Introduction

In spite of the major effort of a large number of investigators, the problem of strong magnetism of the d-metals, and of their alloys and compounds [1–3] is still far from being finally solved. This situation has both a purely theoretical physics aspect (in particular, the problems of the origin of local moments and of the validity of the Fermi

liquid theory and of the quasiparticle description) and a practical one. The theoretical limits on the Curie temperature have not yet been established and the record-high characteristics of soft magnetic materials (such as Permendur) have not been improved significantly for over 50 years [2].

The current status of the theory of the magnetism of metals is such that a more or less consistent description can be provided only for certain classes of magnetic materials. Completely different physical pictures, those of a ferromagnetic Fermi liquid and a state with the Hubbard band splitting and local moments, are used to deal with, respectively, weak itinerant magnets such as ZrZn<sub>2</sub>, Sc<sub>3</sub>In, Ni<sub>3</sub>Al [3] and with ferromagnets of the Fe<sub>1-x</sub>Co<sub>x</sub>S<sub>2</sub> type characterised by a strong electron–electron interaction [4]. In the seventies a fully satisfactory (although semiphenomenological) theory was developed for weak itinerant ferromagnets [3, 5]. With some modifications this theory was subsequently extrapolated to strong itinerant magnets (for example, metals belonging to the iron group) [3], but in general this extrapolation has not been particularly successful [6, 7]. In this situation it would seem very desirable to consider the opposite case of extremely strong magnets with a large spin splitting (compared with the Fermi energy) and very different spin-up and spin-down electron states. The old Stoner theory dealing with ‘strong’ magnets has implied specifically such a situation with a completely filled lower spin subband or a completely empty upper subband. This feature was regarded as applicable to, for example, nickel. Modern calculations of the electron band structure carried out by the spin-density functional method [8] have disproved this picture: the density of the spin-up states  $N_{\uparrow}(E_F)$  is low but finite.

Nevertheless, band calculations carried out from first principles have led to the discovery of a class of real compounds similar to ‘strong’ Stoner ferromagnets. These

V Yu Irkhin, M I Katsnel'son Institute of Metal Physics, Ural Division of the Russian Academy of Sciences, ul. S Kovalevskoi 18, 620219 Ekaterinburg; Tel. (3432)49 91 38; E-mail: ktsn@mik.e-burg.su

Received 4 March 1994

*Uspekhi Fizicheskikh Nauk* 164 (7) 705–724 (1994)

Translated by A Tybulewicz

materials have the Fermi level inside the energy gap of the partial density of states for one of the spin projections. They have therefore been called ‘half-metallic ferromagnets’ (HMFs). De Groot et al. were the first to apply this picture to the Heusler alloys NiMnSb [9] and PtMnSb [9–11] with the  $C1_b$  structure; subsequently, this picture has been applied to CoMnSb [12] and FeMnSb (a half-metallic ferrimagnet) [13]. The state of half-metallic anti-ferro-magnetism was predicted for CrMnSb [11]. Band structure calculations for a large group of ferromagnetic and antiferromagnetic Heusler alloys belonging to a different series with the formula  $T_2MnZ$  ( $T = \text{Co, Ni, Cu, Pd}$ ) and the  $L2_1$  structure have shown [14] that a state close to an HMF with a near zero-density  $N_{\uparrow}(E_F)$  appears in  $\text{Co}_2\text{MnZ}$  systems, where  $Z = \text{Al, Sn}$  (according to Ref. [15], this is also true of the compounds with  $Z = \text{Ga, Si, Ge}$ ). Moreover, the half-metallic state is predicted by calculations of the band structure of  $\text{CrO}_2$  (rutile structure) [16, 17],  $\text{UNiSn}$  ( $C1_b$  structure) [18, 19],  $\text{Fe}_3\text{O}_4$  [11, 20],  $\text{KCrSe}_2$  (see Ref. [21]).

The interest in HMFs has been largely due to the discovery of a giant Kerr rotation of the plane of polarisation in PtMnSb [22] and the concurrent attribution of this effect to the characteristics of the energy spectrum of this HMF [10, 11]. Thus, HMFs are promising magneto-optic recording materials. It is interesting to note that, according to the calculations, the class of HMFs includes such an important magnetic recording material as  $\text{CrO}_2$  (its practical advantages are due not to this aspect, but rather to the good mech-anical adhesive properties of the powder of this material).

It is intuitively clear that HMFs are of interest from the point of view of achieving the maximum saturation magnetisation  $M_0$  (because a further increase in the spin splitting in this state does not increase the magnetic moment). Calculations of the band structure of Fe–Co alloys with record-high values of  $M_0$  for d-systems [23]—which are the basic soft magnetic materials used in modern technology—and of the  $\text{R}_2\text{Fe}_{17}$  and  $\text{R}_2\text{Fe}_{14}$  systems [24–26] (hard magnetic materials), have shown that in a sense these substances resemble HMFs: the Fermi level lies in a deep minimum for one of the spin projections. Such a minimum is typical of systems with local moments and is also exhibited by pure iron. A clear minimum in the density of the spin-down states has also been discovered for the  $\text{RCO}_5$  ( $R = \text{Y, Sm, Gd}$ ) [27] and  $\text{GdNi}_5$  [28] systems. A comparison of the magnetic properties of a large group of  $\text{Y}_n\text{Co}_m$  and  $\text{Y}_n\text{Fe}_m$  alloys with the results of calculations carried out by the simple recursion method is made in Ref. [29]: a state close to an HMF has been found for  $\text{YCo}_5$ ,  $\text{YCo}_7$ , and  $\text{Y}_2\text{Co}_{17}$ .

The density of states  $N_{\uparrow}(E_F)$  in the ferrimagnet  $\text{Mn}_4\text{N}$  is zero for the Mn(I) positions—which make the dominant contribution to the magnetic moment—and has a deep minimum at the Mn(II) positions [30–32], so that this compound should have properties resembling a half-metal. The materials with high values of  $M_0$ , which are of practical importance, include the isostructural ferromagnetic compound  $\text{Fe}_4\text{N}$ , which recently has been the subject of extensive investigations and for which the value of  $N_{\uparrow}(E_F)$  is practically zero at the Fe(I) positions [30, 33] (see also the calculations reported for  $\text{NiFe}_3\text{N}$  [34],  $\text{PdFe}_3\text{N}$  [35]).

All this justifies identification of HMFs as a new class of itinerant ferromagnets with promising practical applications.

Theoretically, the class of HMFs is distinguished primarily by the presence of well-defined local moments and also by the absence of the ‘Stoner continuum’ of the electron–hole excitations and, consequently, by a weak damping of the collective spin-wave throughout the Brillouin zone. This makes them similar to the Heisenberg magnets and also to degenerate ferromagnetic semiconductors [36–39]. The interaction of charge carriers at the Fermi level with well-defined magnons leads to an energy spectrum completely different from the spectrum for the interaction with ‘loosely bound’ paramagnons in weak itinerant magnetic materials [3, 5, 40]. In fact, if the  $\sigma = \uparrow$  subband is filled, the spin-up electrons cannot move freely: they form a very exotic energy band of almost current-free spin-polaron states [40, 41]. This is related to a number of striking experimentally observed anomalies in the spin polarisation of the conduction electrons, in the rate of longitudinal nuclear magnetic relaxation, etc. [36–41]. The spin-polaron effects, due to the scattering of carriers by magnons, are essentially not of the Fermi-liquid nature. They manifest themselves particularly strikingly in HMFs because in the conventional itinerant magnets they are masked by the paramagnon contributions.

This review deals with a whole range of experimental and particularly theoretical problems related to HMFs and also provides an analysis of the importance of these problems in the general theory of itinerant-electron magnetism.

## 2. Band structure and magneto-optic properties

As already pointed out, the most important members of the HMF class are the Heusler alloys  $T_2MnZ$  with the  $L2_1$  structure and  $\text{TMnZ}$  with the  $C1_b$  structure ( $\text{MgAgAs}$ ). The cubic  $L2_1$  structure corresponds to a specific way of filling all four fcc sublattices with T, Mn, and Z atoms, whereas the  $C1_b$  structure differs because one of the sublattices is empty and the crystal symmetry is lowered to tetrahedral (the inversion centre is absent); see Fig. 1.

The formation of the half-metallic state can be generally described as follows [9, 11, 14, 19]. If the hybridisation with

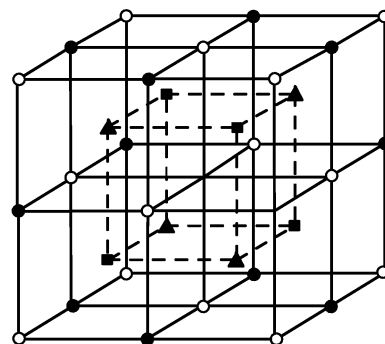


**Figure 1.** Crystal structures of the Heusler alloys, considered as a result of splitting of the fcc lattice into four sublattices. In the  $L2_1$  structure the positions of all three types are filled, whereas in the  $C1_b$  structure the positions identified by the black circles are vacant.

the states of the T and Z atoms is ignored, the d-band of manganese in these structures is characterised by a wide energy gap between the bonding and antibonding states. A strong intra-atomic (Hund) exchange of the manganese ions significantly pushes apart the spin-up and spin-down subbands. One of these spin subbands closely approaches the p-band of the ligands, so that the gap in this subband is smeared out partly or completely by the p-d hybridisation. The gap is retained in the other subband and the Fermi level may be inside it, which gives rise to the HMF state. For example, the calculated band structure of NiMnSb and of a hypothetical compound NiMnSn [42] (the NiMnSb<sub>1-x</sub>Sn<sub>x</sub> system is stable up to  $x \approx 0.7$ ) differ basically only in respect of the Fermi level position relative to the gap of the  $\sigma = \downarrow$  states, which is related simply to the different numbers of the p-electrons in Sb and Sn. On the other hand, the reduction in the number of electrons by one in Co<sub>2</sub>MnZ (Z = Si, Ge) alloys does not shift the gap [15]. However, in the case of the L2<sub>1</sub> structure one should speak rather of a deep pseudogap, whereas in the case of the C1<sub>b</sub> structure it is a real gap. This is due to the considerable change in the nature of the p-d hybridisation (particularly between the p and t<sub>2g</sub> states) when the centre of inversion disappears [9]. The C1<sub>b</sub> structure is therefore more favourable for the appearance of the HMF state.

It follows from Ref. [30] that similar factors are responsible for the gap in the partial density of states at Mn(I), which is one of the manganese positions in the compound Mn<sub>4</sub>N the structure of which can be derived from the T<sub>2</sub>MnZ structure by removal of some atoms. A

qualitatively similar mechanism, based on a strong Hund exchange and on hybridisation of the d-states of chromium with the p-states of oxygen has been discussed [16] for the compound CrO<sub>2</sub> with the rutile structure. It is pointed out in Ref. [14] that the very stability of the ferromagnetic state is a consequence of the difference between the p-d hybridisation in the case of states with different spin projections. The authors of Ref. [14] introduced the term 'covalent magnetism' to describe this situation and stressed the difference from the picture of a spectrum in the simple Stoner model, when the densities of states  $N_{\uparrow}(E)$  and  $N_{\downarrow}(E)$  differ only by a shift equal to the constant spin splitting. The results of the band structure calculations are presented in Figs 2-5.

From the very earliest studies of the electron structure of HMFs particular attention has been paid to the relationship between the structure and the magneto-optic properties. The first studies of HMFs [10, 11] revealed that the major difference between the spin-down and spin-up states near the

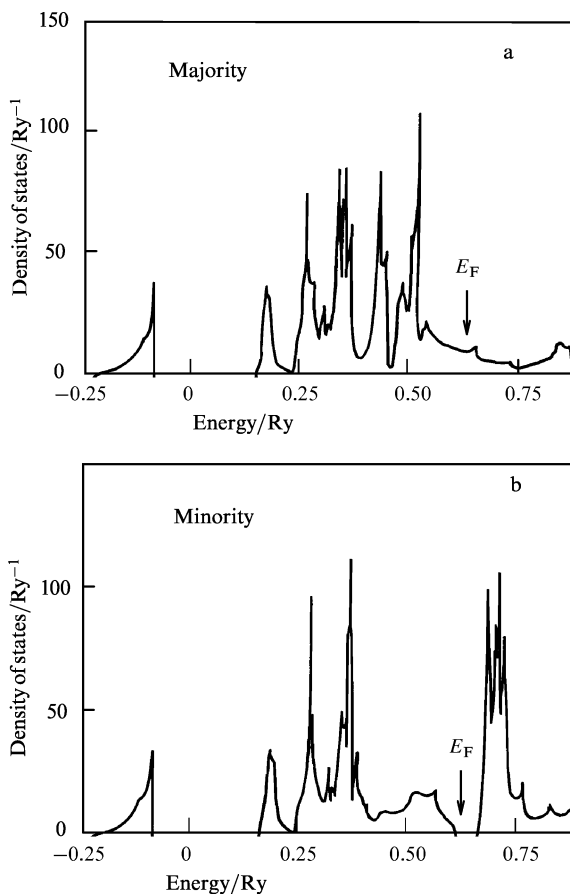


Figure 2. Density of states in PtMnSb [10]: (a) spin-up; (b) spin-down.

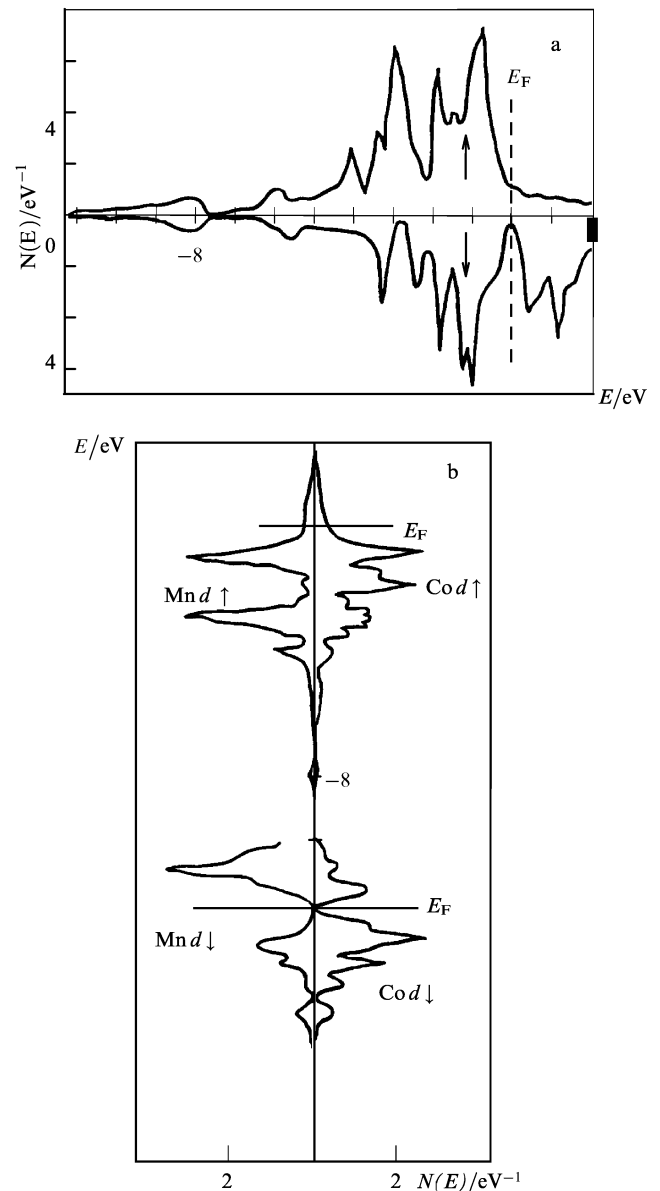


Figure 3. Total (a) and partial (b) densities of states in the Heusler alloy Co<sub>2</sub>MnSn [14].

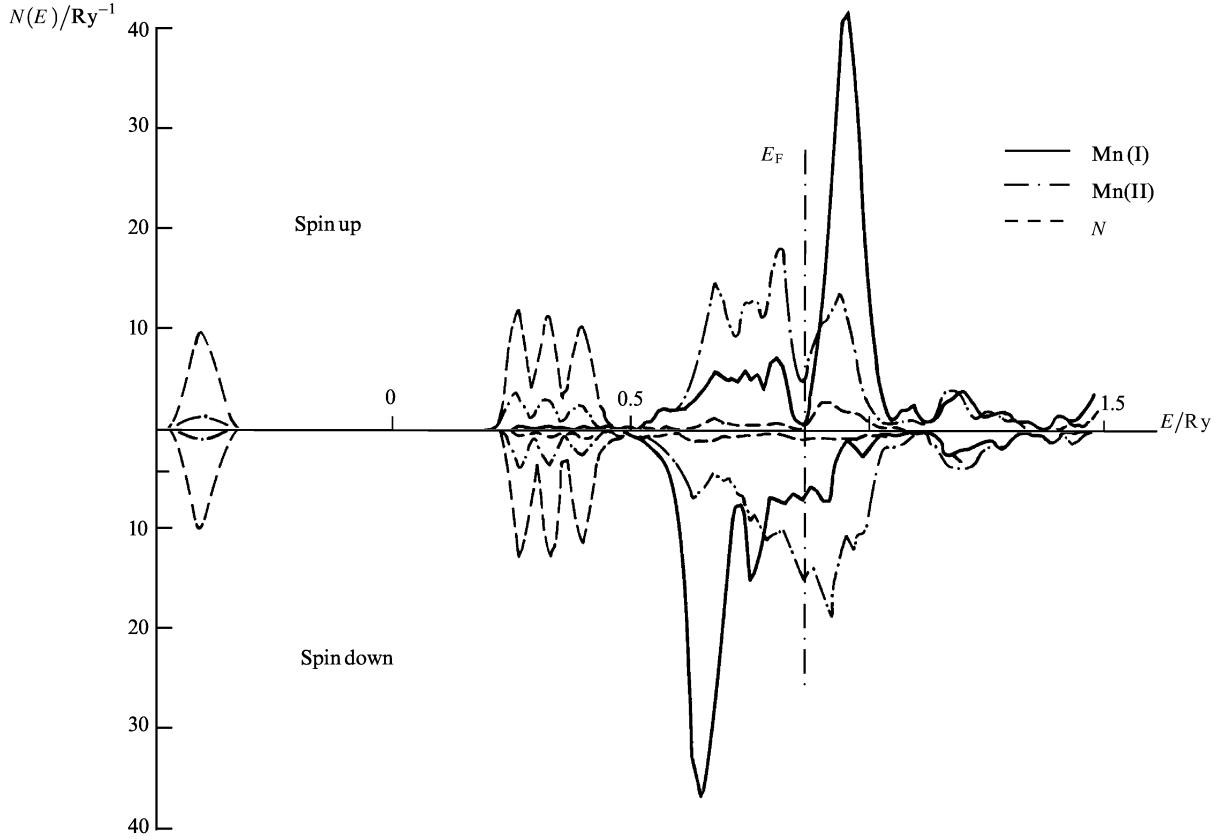


Figure 4. Partial densities of states in  $\text{Mn}_4\text{N}$  [30].

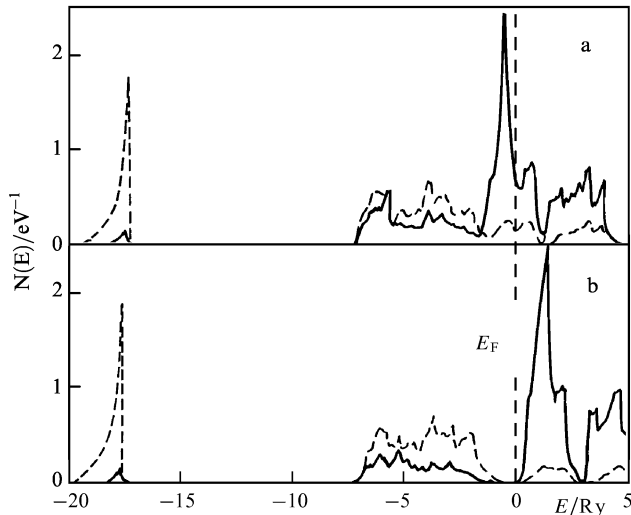


Figure 5. Partial densities of states in  $\text{CrO}_2$  [16]. The continuous curves represent the 3d-states of Cr, whereas the dotted and dashed lines are the 2s- and 2p-states of oxygen. (a) Spin-up; (b) spin-down.

Fermi level gives rise to an asymmetry of the optical transitions and is responsible for the strong Kerr rotation. We shall consider this aspect on the basis of later investigations [19, 43].

Reflection of light of frequency  $\omega$  from a magnetic medium with a complex refractive index  $\tilde{n} = n + ik$  in an off-diagonal conductivity

$$\tilde{\sigma}_{xy} = \sigma_{1xy} + i\sigma_{2xy}$$

alters its plane of polarisation by the Kerr angle

$$\theta_K = \frac{4\pi}{\omega} \frac{A\sigma_{2xy} + B\sigma_{1xy}}{A^2 + B^2}, \quad (2.1)$$

where  $A = n^3 - 3nk^2 - n$ , and  $B = -k^3 + 3n^2k - k$ . Therefore, in the case of weak damping ( $k \ll n$ ) the angle  $\theta_K$  is governed primarily by the quantity  $\sigma_{2xy}$  and the expression for this quantity was derived by Argyres [44]. In the simplest case of a cubic structure with the magnetisation vector parallel to the (001) plane, we have [19]

$$\sigma_{2xy} = \frac{\pi}{\omega} \sum_{\mathbf{k}, m \neq m'} \left\{ F_{m'm'\uparrow}^{xy}(\mathbf{k}) n_{km'\uparrow} (1 - n_{km\uparrow}) \delta[\omega - \omega_{mm'\uparrow}(\mathbf{k})] - F_{m'm'\downarrow}^{xy}(\mathbf{k}) n_{km'\downarrow} (1 - n_{km\downarrow}) \delta[\omega - \omega_{mm'\downarrow}(\mathbf{k})] \right\}, \quad (2.2)$$

where atomic units are used;  $\mathbf{k}$  is the quasimomentum,  $\sigma$  is the spin projection,  $m$  is the band index,  $\omega_{mm'\sigma}(\mathbf{k}) = \varepsilon_{\mathbf{k}m\sigma} - \varepsilon_{\mathbf{k}m'\sigma}$  is the frequency of the interband transitions,  $n_{km\sigma} = f(\varepsilon_{\mathbf{k}m\sigma})$  is the Fermi distribution function

$$F_{m'm'\sigma}^{xy}(\mathbf{k}) = 2i \sum_{m''} \left[ \frac{(L_{m''m}^z)^*}{\omega_{m'm''}} P_{m''m}^x P_{mm'}^y + \frac{L_{m''m}^z}{\omega_{m'm''}} P_{m''m}^x P_{m'm}^y \right], \quad (2.3)$$

$$P_{m'm}^x = \langle m' \mathbf{k} \sigma | -i \frac{\partial}{\partial x} | m \mathbf{k} \sigma \rangle, \quad L_{m'm}^z = \langle m' \mathbf{k} \sigma | \xi L^z | m \mathbf{k} \sigma \rangle, \quad (2.4)$$

$L^z$  is the  $z$ -projection of the orbital momentum operator,  $\xi = (2/rc^2) \partial V_{\text{eff}} / \partial r$ , and  $V_{\text{eff}}$  is the effective potential acting on the conduction electrons.

It is evident from Eqn (2.2) that if the  $\varepsilon_{km\sigma}$  spectrum depends weakly on  $\sigma$  in a layer of thickness  $\omega$  near  $E_F$ , the first and second terms in the curly brackets practically cancel out. On the other hand, in the case of HMFs when  $\omega \leq \Delta_\sigma$  ( $\Delta_\sigma$  is the gap for the spin projection  $\sigma$ ), the corresponding term in Eqn (2.2) vanishes, so that large values of  $\sigma_{xy}$  and of the Kerr rotation can be expected. It is in fact found that the intensities of the peaks in the frequency dependence of  $\theta_K$  for the NiMnSb<sub>1-x</sub>Sn<sub>x</sub> system decrease rapidly when  $x$  is increased, i.e. when the Fermi level leaves the gap [42].

The half-metallic ferromagnet Co<sub>2</sub>MnSn, belonging to the Co<sub>2</sub>YZ Heusler alloy series, has the highest values of  $\sigma_{2xy}(\omega)$  at low frequencies [45] (Fig. 6). On the other hand, the appearance of the energy gap for the spin-down states (not necessarily located at  $E_F$ ) is evidently typical of the whole series. At  $\omega \geq 1.5$  eV (which of the order of a typical separation between the gap and the Fermi level) there are no qualitative differences between Co<sub>2</sub>MnSn and other members of this Heusler alloy series.

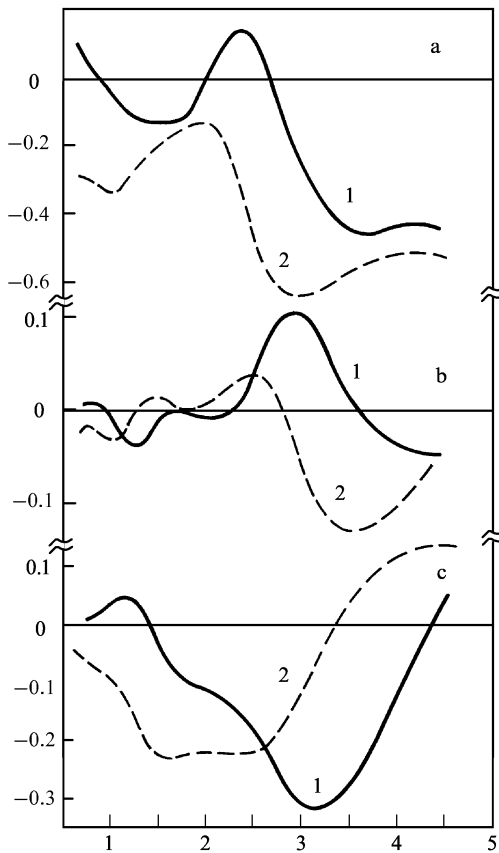


**Figure 6.** Experimental dependences  $\omega^2 \text{Im} \varepsilon_{xy}(\omega)$  (curves labelled 1) and  $-\omega^2 \text{Re} \varepsilon_{xy}(\omega)$  (2) obtained for T<sub>2</sub>MnSn [45]. T = Co (a), Ni (b), and Cu (c).

It follows from Eqn (2.3) that the angle  $\theta_K$  is proportional to the spin-orbit coupling, i.e. it is larger for heavier elements. We can therefore expect that HMFs containing platinum have larger values of  $\theta_K$ . A giant value  $\theta_K \approx 2.5^\circ$  (for red light), much higher than the value for NiMnSb, has been reported for PtMnSb [11, 22] (the results of the calculation are presented in Fig. 7). However, it should be pointed out that, according to Ref. [21], the main

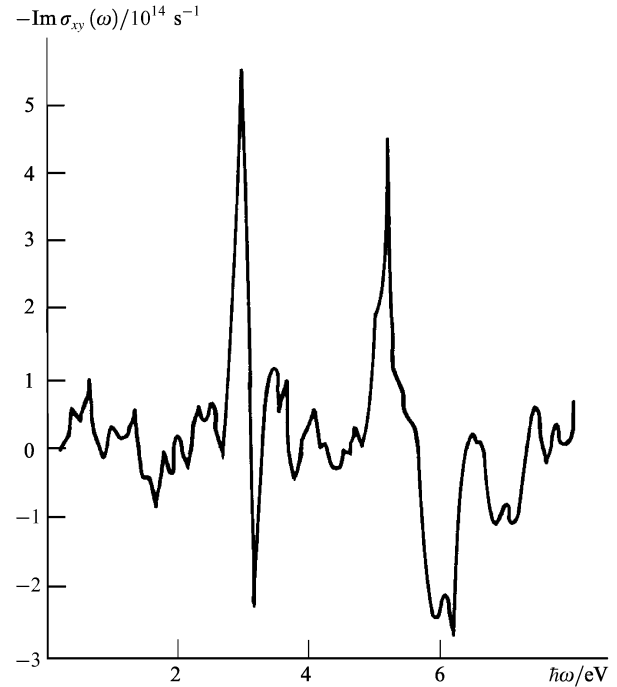


**Figure 7.** Results of calculation of the quantity  $-\text{Im} \sigma_{xy}(\omega)$  (frequency is in electron volts), which governs the Kerr rotation in PtMnSb [19].

difference between the electron band structures of the HMFs PtMnSb and NiMnSb, responsible for the smaller value of  $\theta_K$  in the latter case, is related not so much to the values of the spin-orbit matrix elements, as to the shift of some of the energy levels because of ‘scalar’ relativistic effects (velocity dependence of the mass and the Darwin correction). Therefore, in this respect the simplest assumption of a direct connection between the spin-orbit coupling and the Kerr rotation is not quite adequate.

Record values of  $\theta_K$  might be expected for the ferromagnetic phase of the compound UNiSn [19], but experiments have shown that it is an antiferromagnet [46, 47] (it is discussed in Section 9). Nevertheless, it is interesting to consider the isostructural ferromagnets containing actinides (for example, UCoSn and PdUSn). A first-principles calculation of the magneto-optic properties of CrO<sub>2</sub> [43] gives very moderate values of  $\theta_K$  ( $0.15^\circ$  for visible light), which is due to the smallness of the relativistic effects (light atoms) and, consequently, of the  $F^{xy}$  matrix elements in Eqn (2.2). A comparison of the magneto-optic properties with calculations of the band structure of Fe-Co alloys can be found in Ref. [48].

It is worth considering the question of experimental confirmation of the calculated electron band structure of HMFs. The most direct check of the electron spectrum can probably be provided by investigations of the de Haas-van Alphen effect and a comparison of the experimentally determined Fermi surface with that found by calculation. Unfortunately, the relevant data are not yet available. The results of experimental investigations of the optical properties of NiMnSb and PtMnSb [49], as well as of CrO<sub>2</sub> [50], together with the angle-resolved data on the photoemission from PtMnSb [51] are, according to the authors of these papers, in good agreement with the results of an analysis of the band calculations [9–11, 16] (in some cases it is

necessary to make corrections for the spin–orbit coupling, which is ignored in the calculations).

A paradoxical result follows from the experimental data on the photoemission from CrO<sub>2</sub> [52]: there are no electron states with both spin projections near  $E_F$ , whereas according to all the properties of this compound it is undoubtedly a metal (although with a high electric resistivity). The results reported in Ref. [52] can be explained by, for example, surface effects. An alternative (and more interesting) explanation involves allowance for the final-state effects. The compound CrO<sub>2</sub> is known to be a system with strong electron correlations [53], which is confirmed by, for example, the observation of the ‘Hubbard’ absorption peaks in the optical spectrum [54]. Therefore, the field of a hole, which is formed as a result of the photoemission and interacts strongly with the remaining electrons, may be sufficient for the formation of a localised state. This problem needs further investigation.

### 3. Transport properties and the problem of spin polarisation

In conventional metallic ferromagnets the contribution of the magnetic scattering to the low-temperature transport properties is governed primarily by one-magnon scattering processes. These processes dominate in the temperature range

$$T^* \ll T < T_C, \quad T^* \sim \frac{I^2 S}{E_F^2} T_C, \quad (3.1)$$

where  $I$  is the  $s$ – $d$  exchange parameter. At lower temperatures the contribution of one-magnon processes is exponentially small because electron transitions across the ferromagnetic gap  $\Delta$  are impossible in the range of the thermal magnon momenta. However, since  $|I| \ll E_F$  is usually true, the condition (3.1) covers practically the whole spin-wave temperature range.

Let us consider the contribution made to the resistivity, which appears in the second order in  $I$ . This can be done with the use of the Mori formula [55]. The reciprocal of the transport relaxation time is

$$\frac{1}{\tau} = \int_0^\infty dt \left( [\hat{v}(t), H_{\text{int}}], [H_{\text{int}}, \hat{v}] \right) (\hat{v}, \hat{v})^{-1}, \quad (3.2)$$

where  $H_{\text{int}}$  is the transverse part of the  $s$ – $d$  Hamiltonian describing spin-flip processes,

$$\hat{v} = \sum_{k\sigma} v_{k\sigma} c_{k\sigma}^+ c_{k\sigma}, \quad v_{k\sigma} = \frac{\partial \varepsilon_{k\sigma}}{\partial k}$$

is the velocity operator of the conduction electrons, and

$$(A, B) = \int_0^{1/T} d\lambda \langle A \exp(-\lambda H) B \exp(\lambda H) \rangle.$$

Calculations yield

$$\frac{1}{\tau} = 8\pi I^2 S \left[ \sum_{k,\sigma} v_{k\sigma}^2 \left( \frac{-\partial n_{k\sigma}}{\partial \varepsilon_{k\sigma}} \right) \right]^{-1} \sum_{k,k'} (v_{k\uparrow} - v_{k'\downarrow})^2 \times n_{k\uparrow} (1 - n_{k'\downarrow}) N_{k-k'} \delta(\varepsilon_{k'\downarrow} - \varepsilon_{k\uparrow} - \omega_{k-k'}) \quad (3.3)$$

$[n_{k\sigma} = f(\varepsilon_{k\sigma})$  and  $N_q = N_B(\omega_q)$  are the Fermi and Bose distribution functions, and  $\omega_q$  is the magnon frequency], which generalises the standard result [2] to the case of

arbitrary  $\varepsilon_{k\sigma}$  spectra. The temperature dependence of the resistivity in the range defined by Eqn (3.1) is

$$\rho \propto I^2 N_\uparrow(E_F) N_\downarrow(E_F) \left( \frac{T}{T_C} \right)^2. \quad (3.4)$$

It therefore follows that the contribution described by Eqn (3.4) vanishes in the case of HMFs. Similarly, there is no contribution of one-magnon processes to the anomalous Hall effect  $R_s(T) \propto (aT^3 + bT^4)$  in these materials [2, 56].

It follows that the magnetic scattering in HMFs should be dominated by two-magnon processes. As a rule, these processes give rise to higher power exponents in the temperature dependence, because the resistivity is proportional to  $T^{7/2}$  [2]. Moreover, the relevant contributions are small in terms of formal parameters of the model (for example, in terms of the quasiclassical parameter  $1/2S$ ). We can therefore expect significant singularities in the temperature dependences of the transport properties of HMFs.

Experimental investigations of the dielectric resistivity  $\rho(T)$  and the spontaneous Hall coefficient  $R_s(T)$  of the Heusler alloys TMnSb ( $T = \text{Ni, Co, Pt, Cu, Au}$ ) and PtMnSn are reported in Refs [57, 58]. The contribution of one-magnon processes (which is of the order of  $T^2$ ) to the

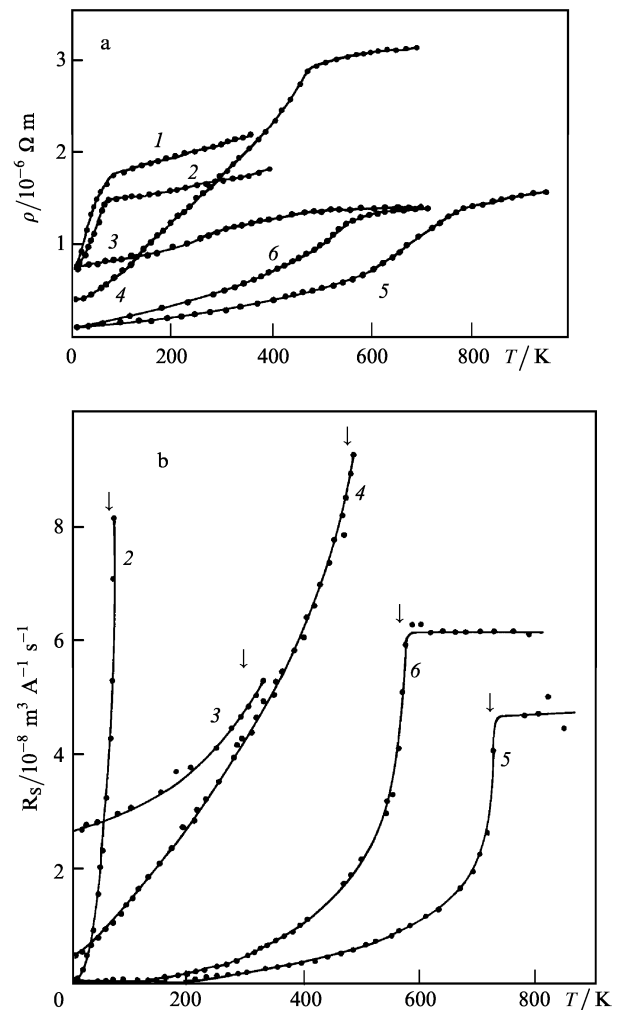


**Figure 8.** Temperature dependences of the electric resistivity (a) and of the spontaneous Hall coefficient (b) of the Heusler alloys TMnSb [ $T = \text{Cu}$  (1), Au (2), Co (3), Ni (4), Pt (5)] and PtMnSn (6) [58].

resistivity of HMFs ( $T = \text{Ni, Co, Pt}$ ) was indeed not detected, whereas in the case of ‘conventional’ ferromagnets the dependences  $\rho(T)$  are much steeper (Fig. 8).

On the other hand, in Refs [57, 58] the observation that the spin polarisation of carriers

$$P(T) = \frac{n_{\uparrow}(T) - n_{\downarrow}(T)}{n_{\uparrow}(T) + n_{\downarrow}(T)}, \quad (3.5)$$

determined from  $R_s(T)$  at moderately low temperatures, is proportional to the magnetisation is considered a problem. At first sight, this result seems to be strange, because the value of  $n_{\downarrow}$  should be independent of temperature right down to  $T_C$  in view of the presence of the energy gap.

In relation to this observation it is interesting to consider the results of direct measurements of  $P(T)$ . The method of spin-polarised photoemission from NiMnSb just gave values of about 50%, instead of the expected 100% polarisation [59]. We shall show later that this conflict can be resolved if allowance is made for the correlation effects.

#### 4. Magnetic properties

Table 1 gives the main magnetic properties of some HMFs and, for comparison, the properties of two ‘conventional’ ferromagnets Pd<sub>2</sub>MnSn and PtMnSn belonging to the T<sub>2</sub>MnZ [60–62] and TMnZ [63] Heusler alloy series. All these systems have high values of the saturation magnetisation and of the Curie temperature. The strong magnetism of the Heusler alloys is mainly due to the local moments of well-separated manganese atoms. For example, the total magnetic moment of Co<sub>2</sub>MnZ,  $(4-5)\mu_B$  per formula unit, consists of the moment  $3\mu_B$  per Mn atom and less than  $1\mu_B$  per Co atom [15]. The relative proximity of the paramagnetic and ferromagnetic Curie temperatures is evidence of the localised nature of the magnetic moments. The values of the effective moments above  $T_C$ , deduced from the Curie constant, decrease quite rapidly when temperature is increased [61–63]. The experimentally determined Wohlfarth–Rhodes ratio  $p_c/p_s$  is considerably less than unity. We recall that in the Heisenberg model we have  $p_c/p_s = 1$  and for weak itinerant ferromagnets the corresponding ratio is  $p_c/p_s \gg 1$  [3]. In the case of ‘conventional’ strong itinerant ferromagnets (for example, Fe and Ni) this ratio is somewhat greater than unity. It therefore follows that

**Table 1.** Values of the magnetic moment  $p_s$  in the ground state, deduced from the saturation magnetisation ( $\mu_0 = p_s\mu_B$ ), the ferromagnetic and paramagnetic Curie temperatures  $T_C$  and  $\theta$ , and the paramagnetic moment  $p_c$  deduced from the Curie constant [ $C = \mu_{\text{eff}}^2/3 = p_c(p_c + 2)\mu_B^2/3$ ], for the Heusler alloys. The range of values of the last two quantities corresponds to a change with increase in temperature.

	$p_s$	$T_C/\text{K}$	$\theta/\text{K}$	$p_c$
Co <sub>2</sub> MnSi	5.10	1034	1044	2.03
Co <sub>2</sub> MnGe	4.66	905	890	2.61
Co <sub>2</sub> MnSn	5.37	826	870	3.35
Co <sub>2</sub> MnGa	4.09	695	770	3.28
CoMnSb	4.2	478	490–520	3.61–3.11
NiMnSb	4.2	728	780–910	3.31–2.06
PtMnSb	3.96	572	610–670	3.96–3.56
Pd <sub>2</sub> MnSn	4.22	189	201	4.05
PtMnSn	3.5	330	350	4.2

the inequality  $p_c < p_s$  is a striking property of HMFs, which could be used in their preliminary identification.

Theoretically the temperature dependence of the magnetic moment is governed by the competition between two opposite trends. The ‘temperature-induced’ moments [3] are most important in the case of weak itinerant magnets, when there are no localised moments in the ground state. In ferromagnets with well-defined local moments another factor comes into play: the moments decrease as a result of misorientation [64, 65]. These calculations demonstrate that the reduction in the moments is a consequence of a change in the electron structure as a result of rotation of the magnetic moments. One would expect such changes to be particularly large in the case of HMFs and they should be of qualitative nature (smearing out of the hybridised gap because of spin disorder). The many-electron mechanism of the suppression of magnetic moments is discussed in the next section. The reduction in the moment with an increase in temperature may also be related to other factors. For example, the difference between  $p_c = 3.4$  and  $p_s = 4.2$  for the Ni<sub>2</sub>MnGa Heusler alloy [66] is attributed to the splitting of the nickel states (owing to the Jahn–Teller band effect related to the transition from the high-temperature cubic phase to the tetragonal phase).

The magnetic properties of CrO<sub>2</sub> have been investigated less than those of the Heusler alloys. Nevertheless, the saturation value of the magnetic moment is very close to the atomic value  $\mu_0 = 2\mu_B$  ( $p_s = 2$ ) in the case of the Cr<sup>4+</sup> ion. This is confirmed by the band structure calculations [16] and is important for itinerant magnets.

As pointed out in the Introduction, an important feature of HMFs is the weak damping of spin waves throughout the Brillouin zone because of the absence of the Stoner continuum. Experimental data are now available on the scattering of neutrons in the Heusler alloys Pd<sub>2</sub>MnSn, Ni<sub>2</sub>MnSn [67], and Cu<sub>2</sub>MnAl [68]. Spin waves are well-defined over the whole Brillouin zone and—according to Ref. [3]—this is the criterion of validity of the model of localised moments. According to the band theory, the weak magnon damping can be explained by the fact that the partial densities of the spin-up d-states of the Mn atoms are low since the corresponding subband is almost filled [14]. The damping may be expected to be even weaker if the Fermi level of one of the spin projections falls within a hybridised gap. Thus, experimental investigation of the damping of spin waves and a comparison with the results for the various Heusler alloys belonging to the T<sub>2</sub>MnZ and TMnZ series would be of great interest for the validation of the theory.

Another physical property in which the distinctive features of HMFs are apparent is the rate of longitudinal nuclear magnetic relaxation  $1/T_1(T)$ . The Korringa contribution of the conduction electrons is the dominant contribution for ‘conventional’ metallic ferromagnets and is described by the Moriya formula [3, 69, 70]:

$$\frac{1}{T_1} = \pi\gamma_n^2 A^2 T F N_{\uparrow}(E_F) N_{\downarrow}(E_F) \quad (4.1)$$

( $\gamma_n$  is the gyromagnetic ratio,  $A$  is the hyperfine interaction constant, and  $F$  is the exchange enhancement factor). Since the contribution represented by Eqn (4.1) vanishes in HMFs (which essentially follows also from the absence of the decay of magnons into Stoner excitations), significant anomalies in the temperature dependence

$1/T_1(T)$  can be expected. (The theoretical dependence, which is  $T^{5/2}$ , is discussed below.) On the other hand, the transverse nuclear relaxation rate includes a contribution of the longitudinal susceptibility and, therefore, of the transitions inside the spin subbands (see Ref. [70]):

$$\frac{1}{T_2} = \frac{1}{2T_1} + \frac{\pi}{2} \gamma_n^2 A'^2 T F' [N_{\uparrow}^2(E_F) + N_{\downarrow}^2(E_F)], \quad (4.2)$$

i.e. the linear Korringa contribution is also present in HMFs. For simplicity, let us ignore the dependences of the matrix elements of the hyperfine interaction on the spin and let us also neglect the exchange enhancement. We then find that

$$\frac{1/T_2}{1/T_1} \approx \frac{[N_{\uparrow}(E_F) + N_{\downarrow}(E_F)]^2}{4N_{\uparrow}(E_F)N_{\downarrow}(E_F)} \geq 1. \quad (4.3)$$

Major deviations from the linear Korringa law have been found experimentally for  $1/T_1$  of the half-metallic ferromagnet NiMnSb [7]. At moderately low temperatures in the range  $T > 250$  K ( $T_C = 750$  K) the dependence is found to be

$$\frac{1}{T_1(T)} = aT + bT^{3.8}.$$

Nuclear magnetic relaxation at the Mn(I) positions has been studied in the ferrimagnet Mn<sub>4</sub>N with  $T_C = 720$  K, discussed above (a narrow NMR line has been reported only for this compound) [72]. At low temperatures  $T < 77$  K the dependence  $1/T_1(T)$  is linear, but at higher temperatures it is approximately quadratic.

The mechanisms of nuclear magnetic relaxation in magnetite Fe<sub>3</sub>O<sub>4</sub> [73], which exhibits the Verwey transition with a strong reduction in the conductivity at  $T = 130$  K, is obviously quite complex. The ‘metallic’ behaviour of the relaxation rates (increase with temperature) occurs above 200 K. The ratio  $(1/T_2)/(1/T_1)$  is approximately 2.

These anomalies of  $1/T_1$  have been reported before the discovery of HMFs and have not been attributed to the characteristics of the electron band structure (which accounts for the attempt made in Ref. [71] to separate the linear term). Therefore, a deliberate investigation of nuclear magnetic relaxation in compounds for which the HMF state is predicted, which would make it possible to check the results of the band calculations, is highly desirable. It follows from Eqns (4.1)–(4.3) that a significant difference between the Korringa contributions to  $1/T_1$  and  $1/T_2$  should also be observed in ‘conventional’ itinerant magnetic materials if near the Fermi level there are density-of-state peaks leading to a large difference between  $N_{\downarrow}(E_F)$  and  $N_{\uparrow}(E_F)$  for the ferromagnetic phase. For example, the value of  $1/T_2$  for iron and nickel is several times greater than  $1/T_1$  [70]. Allowance for the exchange enhancement produces a larger increase in the transverse susceptibility, i.e. it predicts a trend opposite to that observed experimentally.

## 5. Theoretical investigation of the energy spectrum within the framework of the s–d exchange and the Hubbard models: nonquasiparticle states

As pointed out above, a realistic microscopic model of an HMF should allow for the hybridisation of the s(p)- and d-states. The Hamiltonian can then be written in the form

$$H = \sum_{k\sigma} t_k c_{k\sigma}^{\dagger} c_{k\sigma} + E_d \sum_{i\sigma} d_{i\sigma}^{\dagger} d_{i\sigma} + \sum_{k\sigma} V_k (c_{k\sigma}^{\dagger} d_{k\sigma} + d_{k\sigma}^{\dagger} c_{k\sigma}) + U \sum_i d_{i\uparrow}^{\dagger} d_{i\uparrow} d_{i\downarrow}^{\dagger} d_{i\downarrow}. \quad (5.1)$$

The electron and magnon spectra in the spin-wave temperature range have been investigated on the basis of the generalised Anderson model of Eqn (5.1) [74]. However, in a detailed discussion of the correlation effects it is convenient to use the simpler s–d exchange model and the Hubbard model with a nondegenerate conduction band and spin splitting independent of the wave vector. In particular, these models can be derived from Eqn (5.1) by a canonical transformation in the limiting cases when  $V_k = \text{const}$ ,  $E_d \rightarrow -\infty$  and  $t_k = \text{const}$ , respectively.

Calculation of the one-electron Green functions in the spin-wave temperature range, carried out within the framework of the s–d exchange model [2] and in the ‘parquet’ approximation in combination with the diagram technique [75], and by the equation-of-motion method [36–38] gives

$$G_{k\sigma}(E) = [E - t_{k\sigma} - \Sigma_{k\sigma}(E)]^{-1}, \quad (5.2)$$

$$t_{k\sigma} = t_k - \sigma I \langle S^z \rangle, \quad \Sigma_{k\sigma}(E) = \frac{2I^2 \langle S^z \rangle R_{k\sigma}(E)}{1 + \sigma I R_{k\sigma}(E)}, \quad (5.3)$$

$$R_{k\uparrow}(E) = \sum_q \frac{N_q + n_{k+q\downarrow}}{E - t_{k+q\downarrow} + \omega_q}, \quad (5.4)$$

$$R_{k\downarrow}(E) = \sum_q \frac{1 + N_q - n_{k-q\uparrow}}{E - t_{k-q\uparrow} - \omega_q}.$$

These expressions are exact at  $T = 0$  in the limit of zero carrier density, in which the problem can be reduced to the solution of the Schrodinger equation for one electron interacting with localised spins [36, 76]. The half-metallic state is described as a ‘saturated’ ferromagnetic state with a large spin splitting  $|A| = 2|I| \langle S^z \rangle > E_F$ , i.e.  $n_{k\downarrow} = 0$  (or  $n_{k\uparrow} = 0$  in the s–d exchange model with  $I < 0$ ). In the s–d model this situation corresponds in particular to degenerate ferromagnetic semiconductors [37]. Similar results are obtained in the Hubbard mode [40, 77] if  $I$  is replaced with the intra-atomic Coulomb interaction parameter  $U$ . It should be stressed that the Green function of Eqn (5.2), like the Green function in the Hubbard-I approximation [78], gives the correct atomic limit. On the other hand, at low values of  $U$  it correctly reproduces the Hartree–Fock approximation.

Let us now consider the motion of carriers in the Hubbard model with an almost half-filled conduction band in the limit of strong correlations, when—according to the Nagaoka theorem [79]—the ground state for simple lattices is known to be a saturated ferromagnet. The Hubbard Hamiltonian for  $U \rightarrow \infty$  and  $n < 1$ , when the doubly occupied states (‘pairs’) are forbidden, has the following form in the representation by many-electron  $X$  operators  $X_i^{\alpha\beta} = |\alpha\rangle\langle\beta|$ :

$$H = - \sum_{i,j,\sigma} t_{ij} X_i^{0\sigma} X_j^{\sigma 0} = \sum_{k,\sigma} \varepsilon_k X_{-k}^{0\sigma} X_k^{\sigma 0}, \quad (5.5)$$

where  $|\sigma\rangle$  are singly occupied states with the spin projection  $\sigma$  at a site  $i$ ;  $|i0\rangle$  are empty sites (holes), and  $\varepsilon_k = -t_k$ . Let us consider the Green functions



$$\tilde{G}_{k\sigma}(E) = \langle \langle X_k^{\sigma 0} | X_{-k}^{0\sigma} \rangle \rangle_E. \quad (5.6)$$

For  $\sigma = \uparrow$  at  $T = 0$  the carriers travel freely and the temperature corrections to the spectrum are proportional to  $T^{5/2}$ . A more interesting situation is that of  $\sigma = \downarrow$ , in which case the calculation gives [40, 41]

$$\tilde{G}_{k\downarrow}(E) = \left\{ E - \varepsilon_k + \left[ \tilde{G}_{k\downarrow}^{(0)}(E) \right]^{-1} \right\}^{-1}, \quad (5.7)$$

$$\tilde{G}_{k\downarrow}^{(0)}(E) = \sum_q \frac{N_q + n_{k+q}}{E - \varepsilon_{k+q} + \omega_q}, \quad (5.8)$$

and  $n_k = \langle X_{-k}^0 X_k^{+0} \rangle = f(\varepsilon_k)$ . The result given by Eqn (5.7) is identical with Eqn (5.2) in the limit  $U \rightarrow \infty$  if we change from electrons to holes.

Eqn (5.8) defined the Green function of the lowest order in  $c = 1 - n$ , so that the electron states are described formally by a branch cut and is of nonband (free of poles) nature. This applies also to the complete Green function (5.7), because at low values of  $c$  it does not have poles below  $E_F$  on the real axis. The corresponding one-particle distribution function depends weakly on  $\mathbf{k}$ :  $\langle X_{-k}^0 X_k^{-0} \rangle \approx c$ . The states which have this property do not carry an electric current, which follows from a general analysis of the effect of an electric field on the many-electron system [80] (see also an explicit estimate of the mobility in Ref. [41]). These nonquasiparticle states make no contribution to the density of states at  $E_F$  when  $T = 0$ . However, we shall show later that they do contribute to the linear term in the electronic specific heat. Similar properties [apart from the condition  $\delta N(E_F) = 0$ ] have been postulated by Anderson for spinons, which are neutral Fermi excitations in the resonating valence bond (RVB) state that does not have a long-range magnetic order (in the zero-gap variant of the RVB theory). According to Ref. [81], spinons may be described by a Green function with zero residue. In fact, we have demonstrated earlier the existence of such states in a narrow-gap Hubbard ferromagnet.

As  $c$  increases, the Green function of Eqn (5.7) acquires a real pole of the spin-polaron type below  $E_F$ , so that the saturated ferromagnetism is destroyed [77]. The problem of evolution of the magnetic state is fairly complex. In particular, an analysis of higher orders in the gas approximation and the diagram technique have been used [82] to predict an antiferromagnetic instability. The interpolation description, discussed in Section 7, predicts a transition to an unsaturated ferromagnetic state and the nature of the spin-down states changes: they are now described roughly by the Hubbard-I approximation [78]

$$\tilde{G}_{k\sigma}(E) = (n_0 + n_\sigma) [E - (n_0 + n_\sigma)\varepsilon_k]^{-1}, \quad n_\alpha = \langle X_i^{\alpha\alpha} \rangle, \quad (5.9)$$

i.e. they form quasiparticle-type bands of reduced width.

The temperature dependence of the magnetisation

$$\langle S^z \rangle = S - \sum_p N_p$$

and the neglect, for simplicity, of the ‘parquet’ denominators in Eqn (5.3) (more rigorous calculations are reported in Refs [36, 37]) yield the correction to the electron spectrum:

$$\delta E_{k\sigma} = \sigma I \sum_q \frac{t_{k+q} - t_k}{t_{k+q} - t_k + \sigma \Delta} N_q \propto \left( \frac{T}{T_C} \right)^{5/2}. \quad (5.10)$$

On the other hand, the residues of the one-electron Green function

$$Z_{k\sigma} = \left[ 1 - \frac{\partial}{\partial E} \text{Re} \Sigma_{k\sigma}(E) \Big|_{E=\varepsilon_{k\sigma}} \right]^{-1} \quad (5.11)$$

exhibit the stronger dependence  $T^{3/2}$  (exactly the same as in the case of the magnetisation), which occurs in the partial spin densities of states and in the occupation numbers. Expansion of the Dyson equation (5.2) gives

$$N_\sigma(E) = -\frac{1}{\pi} \text{Im} \sum_k G_{k\sigma}(E) = \rho_\sigma(E) - \sum_k \delta'(E - t_{k\sigma}) \times \text{Re} \Sigma_{k\sigma}(E) - \frac{1}{\pi} \sum_k \frac{\text{Im} \Sigma_{k\sigma}(E)}{(E - t_{k\sigma})^2}, \quad (5.12)$$

where

$$\rho_\sigma(E) = \sum_k \delta(E - t_{k\sigma})$$

is the density of states in the Hartree–Fock–Slater approximation. The third term in Eqn (5.12), which arises from the branch cut of the self-energy, describes an incoherent contribution of nonquasiparticle states  $\delta N_\sigma(E)$  owing to the electron–magnon scattering. We can easily see that this contribution differs from zero in the range of energies corresponding to the spin subband with the opposite spin projection  $-\sigma$ . It follows that the density of states under discussion differs greatly from the Stoner density. If only the magnon contributions are retained, then—to within terms of the order of  $T^{3/2}$  in the leading order in  $1/2S$ —the electron occupation numbers [37] are given by

$$\langle c_{k\sigma}^+ c_{k\sigma} \rangle \approx \frac{S + \langle S^z \rangle}{2S} n_{k\sigma} + \frac{S - \langle S^z \rangle}{2S} n_{k, -\sigma}. \quad (5.13)$$

We can see that in spite of the spin splitting, the electron occupation numbers have a strong temperature dependence  $T^{3/2}$ , in contrast to the exponential dependence predicted by the Stoner theory. Formally, contributions of the order of  $T^{3/2}$  appear both because of the temperature dependence of the residues of the Green functions and because of the appearance of nonquasiparticle states in the ‘foreign’ subband.

We can now solve the problem of the spin polarisation in an HMF postulated above. The strong temperature dependence of the residue of the Green function of the lower spin subband and the increase (with temperature) of the ‘tail’ of the nonquasiparticle states in the upper spin subband (Fig. 9) gives rise to the dependence  $P(T) \propto \langle S^z \rangle$  in Eqn (3.5). In the usual Hubbard model this result is trivial because the electrons responsible for the magnetic moment simultaneously form the band structure near the Fermi level. However, it applies also to the s–d(f) model when the carriers and the magnetic moments belong to different energy bands, which is true—for example—of ferromagnetic semiconductors [37, 83, 84] for which such a dependence  $P(T)$  has been observed in field emission experiments [85].

The resistivity and the Hall effect data discussed above [57, 58] demonstrate that the spin polarisation in the Heusler alloys does indeed behave as the relative magnetisation. It has therefore been concluded on the basis of these data that the Heusler alloy should be described by the strong coupling model (when carriers

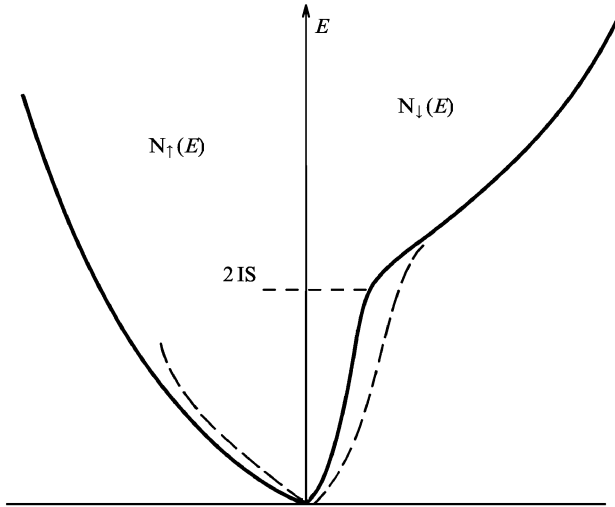


**Figure 9.** Density of states in the  $s$ - $d$  model for an empty conduction band ( $I > 0$ ). At  $T = 0$  (continuous curve) the spin-polaron tail of the spin-down states extends to the bottom of the band. The dashed curve corresponds to finite temperatures.

are coupled strongly to the local moments). It follows from our analysis that this hypothesis is not essential.

The problem of possible depolarisation of the conduction electrons in half-metallic ferromagnets at  $T = 0$  is more difficult. Let us consider the behaviour of the spin polarisation

$$P(E) = \frac{|N_{\uparrow}(E) - N_{\downarrow}(E)|}{|N_{\uparrow}(E) + N_{\downarrow}(E)|} \quad (5.14)$$

on the basis of the  $s$ - $d$  model. If the magnon frequencies in the denominator of Eqn (5.4) are ignored, the presence of the Fermi functions means that the partial density of states with the 'incorrect' spin projection  $\sigma = -\text{sgn } I$  should appear abruptly above ( $I > 0$ ) or below ( $I < 0$ ) the Fermi level (Figs 10 and 11). Allowance for the magnon frequencies  $\omega_q = Dq^2$  smears out this singularity in an interval governed by the maximum magnon frequency. If  $|E - E_F|$  is small compared with  $\bar{\omega} = D(6\pi^2/v_0)^{2/3}$  ( $v_0$  is the unit-cell volume), then [37, 77]

$$\frac{N_{-\alpha}(E)}{N_{\alpha}(E)} = \frac{1}{S} \left| \frac{E - E_F}{\bar{\omega}} \right|^{3/2} \theta[\alpha(E - E_F)], \quad \alpha = \text{sgn } I, \quad (5.15)$$

where  $\theta(x)$  is the Heaviside step function. Away from  $E_F$  the quantity given by Eqn (5.15) becomes a constant, proportional to  $I^2$  in the weak  $s$ - $d$  exchange case (an estimate for ferromagnetic semiconductors gives  $1 - P \approx 4\%$  [84]). In the strong coupling limit, when  $|I| \rightarrow \infty$ , we obtain

$$\frac{N_{-\alpha}(E)}{N_{\alpha}(E)} = \frac{1}{2S} \theta[\alpha(E - E_F)], \quad |E - E_F| \gg \bar{\omega}. \quad (5.16)$$

It therefore follows that the spin polarisation  $P(E)$  changes strongly near the Fermi level. In the case of the antiferromagnetic  $s$ - $d$  exchange there are occupied non-quasiparticle states near  $E_F$ , so that the depolarisation may be detected from the photoemission measurements. If  $I > 0$ , nonquasiparticle states are empty and can be observed in the inverse photoemission experiments.

In the 'wide-band' Hubbard model at  $T = 0$  the nonquasiparticles lie, as in the  $s$ - $d$  model with  $I > 0$ ,

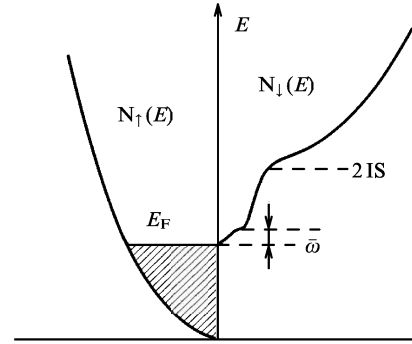


**Figure 10.** Density of states in a half-metallic ferromagnet with  $I > 0$ . The nonquasiparticle states with  $\sigma = \downarrow$  are absent below the Fermi level.

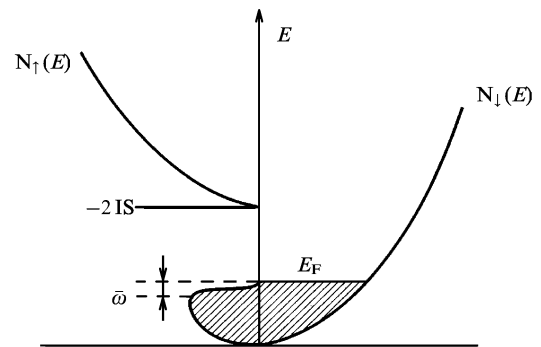


**Figure 11.** Density of states in a half-metallic ferromagnet with  $I < 0$ . The non-quasiparticle states with  $\sigma = \uparrow$  appear below the Fermi level.

above the Fermi level, so that there is no depolarisation of the occupied states. However, the situation changes in the narrow-band limit ( $U \rightarrow \infty$ ). For clarity, let us consider a band with the population  $n > 1$  and the concentration of 'pairs'  $c = n_2 = n - 1 \ll 1$ . The charge carriers are then zero-spin pairs and the spin-up and spin-down electrons may be 'extracted' in the emission experiments with equal probability. On the other hand, it follows from the Pauli principle that the pair states above the Fermi level can be filled only by spin-down electrons. These conclusions are supported by direct calculations of one-particle Green functions [41] [compare with Eqn (5.8) for the case when  $0 < 1 - n \ll 1$ ]. The result is

$$N_{\uparrow}(E) = \sum_{k,q} f(t_{k+q}) \delta(E - t_{k+q} + \omega_q) = \begin{cases} N_{\downarrow}(E), & E_F - E \gg \bar{\omega}, \\ 0, & E > E_F, \end{cases} \quad (5.17)$$

which agrees with Eqn (5.15) for  $\alpha = -$  and  $S = \frac{1}{2}$ . We can see that below  $E_F$  there is no spin polarisation, with the exception of a narrow layer of width  $\bar{\omega}$ , so that experiments carried out with a moderately high energy resolution should yield small values of  $P$ . The real values of the model parameters are obviously intermediate between the broad-band and narrow-band cases, so that significant deviations of  $P(T = 0)$  from 100% are, more generally speaking, not surprising. Inclusion of surface effects does not qualitatively alter the role of the nonquasiparticle contribution to  $P(E)$  [124].

Calculation of the commutator magnon Green function gives [40, 86]

$$\begin{aligned} \langle\langle b_q | b_q^+ \rangle\rangle_\omega &= \left[ \omega - I \sum_k \frac{t_{k+q} - t_k - \omega}{t_{k+q} - t_k + \Delta - \omega} \right. \\ &\quad \left. \times (n_{k\uparrow} - n_{k+q\downarrow}) - \Pi_q^{(2)}(\omega) \right]^{-1}, \end{aligned} \quad (5.18)$$

where the contribution of the two-magnon processes to the polarisation operator is

$$\begin{aligned} \Pi_q^{(2)}(\omega) &= I^2 \sum_{k,p} \left( \frac{t_{k+q} - t_k - \omega}{t_{k+q} - t_k + \Delta - \omega} \right)^2 \\ &\quad \times [B(\mathbf{k}\uparrow, \mathbf{k} + \mathbf{q} - \mathbf{p}\uparrow, \omega_p - \omega) \\ &\quad + B(\mathbf{k} + \mathbf{p}\downarrow, \mathbf{k} + \mathbf{q}\downarrow, \omega_p - \omega) \\ &\quad - B(\mathbf{k} + \mathbf{p}\downarrow, \mathbf{k}\uparrow, \omega_p) \\ &\quad - B(\mathbf{k} + \mathbf{q}\downarrow, \mathbf{k} + \mathbf{q} - \mathbf{p}\uparrow, \omega_p)], \end{aligned} \quad (5.19)$$

The damping of spin waves owing to one-magnon processes is governed by the imaginary part of the second term in square brackets in Eqn (5.18):

$$\begin{aligned} \gamma_q^{(1)}(\omega) &\approx \pi I \Delta \omega \sum_k \left( -\frac{\partial n_{k\uparrow}}{\partial \varepsilon_{k\uparrow}} \right) \delta(\omega - t_{k+q\downarrow} + t_{k\uparrow}) \\ &= 2\pi I^2 S \omega N_\uparrow(E_F) N_\downarrow(E_F) \theta(\omega - \omega_-), \end{aligned} \quad (5.20)$$

where  $\omega$  is the threshold frequency governed by the condition of entry to the Stoner continuum. The damping of magnons at  $T = 0$  gives rise to a logarithmic contribution to the magnon distribution function and, consequently, to the ground-state magnetisation

$$\begin{aligned} \delta \langle S^z \rangle &= -\frac{1}{\pi} \sum_q \int_{-\infty}^0 \frac{\gamma_q^{(1)}(\omega) d\omega}{(\omega - \omega_q)^2 + [\gamma_q^{(1)}(\omega)]^2} \\ &\approx -2I^2 S N_\uparrow(E_F) N_\downarrow(E_F) \ln \frac{W}{\bar{\omega}}, \end{aligned} \quad (5.21)$$

where  $W$  is of the order of the band width. It is shown in detail in Refs [87–90] that this suppression of the moment is similar to the Kondo compensation in the case of a single impurity and that the spin dynamics results in the cutoff of the logarithmic divergences at some characteristic magnon energy  $\bar{\omega}$  rather than at some temperature. This moment-suppression mechanism operates not only in Kondo systems, but also in any magnetic materials with local moments, including those described by the Hubbard model.

Eqn (5.20) for an HMF vanishes and the magnon damping is governed by the imaginary part of Eqn (5.19). Integration yields [86, 91]

$$\gamma_q^{(2)}(\omega_q) = \frac{q^4 v_0^2 (k_{F\uparrow}^2 + k_{F\downarrow}^2)}{48\pi^3 \langle S^z \rangle^2} \times \begin{cases} \frac{\omega_q}{35}, & T \ll \omega_q, \\ \frac{T}{4} \left( \ln \frac{T}{\omega_q} + \frac{5}{3} \right), & T \gg \omega_q. \end{cases} \quad (5.22)$$

The damping of Eqn (5.22) is very weak, as shown both by the numerical values and by the formal parameters. It can be shown [39] that such damping does not alter the magnetisation at  $T = 0$  but simply renormalises the  $T^{3/2}$  Bloch term.

It follows that, in contrast to ‘conventional’ itinerant ferromagnets, the ‘Kondo’ compensation of the moment in an HMF does not occur in the ordered phase (more exactly, the logarithms are cut off at the width of the energy gap). One can expect the situation to apply also above  $T_C$  if there

is a sufficiently strong short-range magnetic order and the electron structure changes only slightly at  $T_C$ . But, at sufficiently high temperatures  $T$  the ‘local’ densities of states  $N_\sigma(E)$  should become comparable and this should result in a fairly major reduction in the magnetic moment of the type described by Eqn (5.21). This mechanism may contribute to a reduction in the effective moment with temperature, observed already for the Heusler alloys (see Section 4).

The real part of Eqn (5.18) determines not only the spin-wave contributions of the order of  $T^{5/2}$ , but also the nonanalytic many-electron correction to the spin-wave stiffness constant [39, 40]. For the quadratic dispersion law  $t_k = k^2/2m$ , we have

$$\begin{aligned} \delta D &= \left( \frac{\pi v_0}{12m \langle S^z \rangle} \right)^2 \frac{T^2}{D} \left\{ [N_\uparrow^2(E_F) + N_\downarrow^2(E_F)] \ln \frac{T}{\omega_+} \right. \\ &\quad \left. - 2N_\uparrow(E_F) N_\downarrow(E_F) \ln \frac{\max(\omega_-, T)}{\omega_+} \right\}, \\ \omega_\pm &= D(k_{F\uparrow} - k_{F\downarrow})^2. \end{aligned} \quad (5.23)$$

This correction predominates over the correction due to the temperature dependences of the Fermi functions, of the order of  $T^2$ , and is particularly large for HMFs.

We now consider the longitudinal nuclear relaxation rate [3]

$$\frac{1}{T_1} = -\frac{A^2 T}{2\pi\omega_n} \text{Im} \sum_q \langle\langle S_q^+ | S_{-q}^- \rangle\rangle_\omega \quad (5.24)$$

( $\omega_n \ll T$  is the NMR frequency). For HMFs we have to consider the contribution of the two-magnon processes (5.18). In the Hubbard model ( $I \rightarrow U$ ), we obtain [40, 92]

$$\begin{aligned} \frac{1}{T_1} &= -\frac{A^2 \langle S^z \rangle}{\pi\omega_n} \sum_q \text{Im} \frac{\Pi^{(2)}(\mathbf{q}, \omega_n)}{\omega_q^2} \\ &= \frac{12\sqrt{\pi}}{\langle S^z \rangle} \left( \frac{v_0}{16\pi^2} \right)^2 \zeta \left( \frac{3}{2} \right) (k_{F\uparrow}^2 + k_{F\downarrow}^2) \frac{T^{5/2}}{D^{7/2}}. \end{aligned} \quad (5.25)$$

The temperature dependence  $T^{5/2}$  can be understood qualitatively on the basis of the Moriya formula (4.1) if  $N_\downarrow(E_F)$  in this formula is replaced with the thermal value of the density of nonquasiparticle states, which is of the order of  $T^{3/2}/D^{3/2}E_F$ . On the other hand, the coefficient in Eqn (5.25) is significantly influenced not only by the values of the density of states, but also by the exchange enhancement factor  $F$ , which in this case is governed by the contribution of the collective magnon mode (this should be compared with the case of weak itinerant magnetic materials, discussed in Ref. [3], when the paramagnon enhancement also leads to  $F \gg 1$ ). It follows that the longitudinal nuclear relaxation rate in an HMF should be regarded, together with the spin polarisation of the emitted electrons, as one of the properties that are governed essentially by nonquasiparticle states.

## 6. Nonquasiparticle contributions to electronic specific heat and transport properties

In the phenomenological theory of a ferromagnetic Fermi liquid [93] and in the standard Fermi liquid theory [94] it is assumed that many-electron effects simply renormalise the density of states  $N(E_F)$  and the Fermi liquid parameters. Let us consider the contribution of spin fluctuations to the specific heat of a ferromagnet. It follows from Eqns (5.11)

and (5.3) that renormalisation of the effective mass and, consequently, of the specific heat in the Hubbard model is described by [40]

$$\frac{m_\sigma^*}{m_\sigma} = \frac{1}{Z_{k_F\sigma}} = 1 + U\Delta \frac{N_{-\sigma}(E_F)}{\omega_+ - \omega_-} \ln \frac{\omega_+}{\omega_-} \quad (6.1)$$

[the notation is the same as in Eqn (5.23)]. In particular, for a weak itinerant magnet, we have

$$\ln \frac{\omega_+}{\omega_-} \approx -2 \ln \alpha, \quad 0 < \alpha = UN(E_F) - 1 \ll 1, \quad (6.2)$$

and Eqn (6.1) describes the paramagnon enhancement. There is no such enhancement in the case of an HMF. It is found that the electronic specific heat of conducting ferromagnets includes contributions of a completely different type, which are of nonquasiparticle origin [40].

It follows from the s-d model that

$$\begin{aligned} C(T) &= \frac{\partial \langle H \rangle}{\partial T} = \frac{\partial}{\partial T} \int dE E f(E) N(E) \\ &= \frac{\pi^2}{3} N(E_F) T + \int dE E f(E) \frac{\partial N(E, T)}{\partial T}. \end{aligned} \quad (6.3)$$

The first term in Eqn (6.3) is the standard result for the electronic specific heat; the second term is due to the temperature dependence of the density of states. Substituting Eqn (5.3) into the last term of Eqn (5.12), we find that

$$\delta C_\sigma(T) = 2I^2 \langle S^z \rangle \sum_{kq} \frac{\sigma f(t_{k+q, -\sigma} - \sigma \omega_q)}{(t_{k+q, -\sigma} - t_{k\sigma})^2} \frac{\partial}{\partial T} n_{k+q, -\sigma}. \quad (6.4)$$

(We recall that in the Hubbard model  $I \rightarrow U > 0$ .) At low temperatures we have

$$f(t_{k+q\downarrow} - \omega_q) = 1, \quad f(t_{k+q\uparrow} + \omega_q) = 0. \quad (6.5)$$

It follows that the nonquasiparticle states with  $\sigma = \downarrow$  do not contribute to the linear term in the specific heat, because these states are empty at  $T = 0$ . For  $\sigma = \uparrow$ , we obtain

$$\delta C_\uparrow = \frac{2\pi^2}{3} I^2 \langle S^z \rangle N_\downarrow(E_F) T \sum_k \frac{1}{(t_{k\uparrow} - E_F)^2}. \quad (6.6)$$

Note that the contribution described by Eqn (6.6) implies that the Fermi liquid description is insufficient only in the case of dynamic quasiparticles defined in terms of the Green-function poles. On the other hand, the entropy of fermions interacting at low temperatures  $T$  can be rigorously described in terms of the distribution functions of Landau quasiparticles with a spectrum defined as the variational derivative of the total energy. The anomalous term in the specific heat is governed by the difference between the spectrum of statistical and dynamic quasiparticles. For the paramagnetic phase this term occurs in the third order in  $U$  [95].

The nonquasiparticle contributions can be separated most readily for a saturated ferromagnet. In the s-d model with  $I < 0$ , when  $N_\uparrow(E_F) = 0$ , Eqn (6.6) gives the sole contribution of the spin-up states to the specific heat. In the s-d model with  $I > 0$  and in the Hubbard model [ $N_\downarrow(E_F) = 0$ ] the nonquasiparticle contributions are absent. It is more difficult to consider the unsaturated case because the density of states with the spin projection

corresponding to the upper spin subband contains, below  $E_F$ , contributions both from poles and branch cuts.

The situation in a Hubbard ferromagnet changes in the case of an almost half-filled band with strong correlations ( $U \rightarrow \infty$ ). In this case it is necessary to adopt the hole representation (or the 'pair' representation for  $n > 1$ ) and the Hubbard model has properties similar to those of the s-d model with  $I < 0$ . Nonquasiparticle 'hole' states, described by the creation operators  $X^{0-}$ , are occupied and if the ferromagnetism is saturated, they are the only states with  $\sigma = \downarrow$  that contribute to the linear specific heat, since the corresponding one-particle Green function has no poles inside the Fermi surface of holes.

Let us first consider the nonquasiparticle contribution to  $C$  on the basis of perturbation theory in terms of  $1/z$  when the Hubbard-I Green functions of Eqn (5.9) are used as the zeroth approximation. If the corrections to the Green functions are found and  $\langle H \rangle$  is differentiated with respect to  $T$ , then for  $U \rightarrow \infty$  and  $n < 1$ , we obtain [40]

$$\delta C_\downarrow = \frac{\pi^2}{3} \frac{4E_F^2 \langle S^z \rangle N_\uparrow(E_F) T}{(n_0 + n_-)(n_0 + n_+)^2} \sum_k \frac{1}{[\varepsilon_k(n_0 + n_-) - E_F]^2}, \quad (6.7)$$

which resembles, in respect of its structure, the result given by Eqn (6.6). For finite values of  $U$  the structure of the spectrum becomes more complex in the presence of the Hubbard subbands and then the nonquasiparticle contributions to the Green functions appear even for the paramagnetic phase. The Hubbard splitting (which, like the spin splitting, is due to the interaction with the local magnetic moments, is in conflict with the standard Fermi liquid theory [6, 7]) may thus lead to the appearance of unusual contributions to the specific heat.

We have seen earlier that the one-particle Green function for the saturated ferromagnetic state can be calculated more rigorously when the concentration of holes  $c$  is low. The contribution to the specific heat is then obtained by expanding Eqn (5.7) in  $G^{(0)}$ . An estimate yields [40]

$$\delta C_\downarrow(T) \propto Tc^{-1/3} \ln \frac{1}{c}, \quad \delta C_\downarrow(T) \gg \delta C_\uparrow(T) \propto Tc^{1/3}. \quad (6.8)$$

The increment in the specific heat described by Eqn (6.8) is somewhat less than for the paramagnetic state when the Gutzwiller method yields an increment of the order of  $1/c$  [96]. Nevertheless, in the limit of small values of  $c$  the contribution of low-mobility nonquasiparticle states to the specific heat predominates. Here once again, we may recall the analogy with the Anderson spinons [81], which do not carry an electric charge, but are responsible (in the zero-gap variant of the RVB theory) for the linear specific heat.

This mechanism of the increase in the specific heat should be the dominant one in HMFs, and in the case of 'conventional' strong ferromagnets should exist alongside the 'paramagnon' mechanism. It is worth mentioning the data on  $Mn_4N$ : the experimental value of the electronic specific heat of this compound is several times greater than the theoretical value deduced from the band structure calculations [31]. This is true also of the Heusler alloys  $X_2MnSn$  and  $X_2MnI$  [97] and the authors of this paper directly attribute the observed specific heat increment to spin fluctuations.

We shall now consider the nonquasiparticle contributions to the transport properties within perturbation theory.

It is shown in Section 3 that the contribution of the  $s$ - $d$  scattering to the electric resistivity, associated with the nonquasiparticle states, is missing in the second order in  $I$ . This contribution does however appear in the presence of impurity scattering [98]. Let us expand the electron Green function to second order in the impurity potential  $V$ :

$$\begin{aligned} \langle\langle c_{k\sigma} | c_{k'\sigma}^+ \rangle\rangle_E &= \delta_{kk'} G_{k\sigma}(E) \\ &+ V G_{k\sigma}(E) G_{k'\sigma}(E) \left[ (1 + V \sum_p G_{p\sigma}(E)) \right] \end{aligned} \quad (6.9)$$

(the  $G$ s are the exact Green functions for an ideal crystal). The transport relaxation time, deduced without the vertex corrections, is then found from the imaginary part of the  $T$  matrix:

$$\tau_\sigma^{-1}(E) = 2\pi V^2 N_\sigma(E). \quad (6.10)$$

Allowance for the energy dependence of the nonquasiparticle contribution to the density of states near  $E_F$  [Eqn (5.15)] yields the corrections to the electric conductivity

$$\delta\sigma \propto -V^2 \int dE \left[ -\frac{\partial f(E)}{\partial E} \right] \delta N(E) \propto -T^{3/2}. \quad (6.11)$$

Since the correction (5.15) contains a contribution which is odd in terms of  $E - E_F$ , there are also contributions to the thermoelectric power of the order of  $T^{3/2}$ .

A detailed analysis of the nonquasiparticle contributions to the transport properties is an interesting and difficult task. As in the case of NMR considered in the preceding section, the contribution of the two-magnon processes to the resistivity of the order of  $T^{7/2}$  can be attributed to the scattering into nonquasiparticle states.

## 7. Ferromagnetism of systems with strong correlations

One of the fundamental problems in the theory of strong magnetism of itinerant electrons is the description of the formation of local magnetic moments and the explanation of the Curie–Weiss law. Although the spin-fluctuation theories [3] and the band structure calculations [64] have resulted in some progress, the local moments in such theories are still introduced largely in an ad hoc manner because the initial translation-invariant system is replaced by a disordered system with random magnetic fields.

The most difficult case to treat by the spin-fluctuation approach or by the standard band calculations is that of itinerant magnetic materials with strong electron–electron correlations (when the intra-atomic interaction parameter is not small compared with the width of the conduction band). In this case the correlations may induce a radical modification of the electron spectrum: the Hubbard subbands may form [78].

According to Mott [53], the Hubbard splitting occurs in some antiferromagnetic oxides and sulfides, and in some metallic ferromagnets such as  $\text{CrO}_2$ , and in the  $\text{Fe}_{1-x}\text{Co}_x\text{S}_2$  system of solid solutions with the pyrite structure. Such solid solutions represent an ideal model system for a theoretical investigation of ferromagnetism in the state with the Hubbard subbands. Its electron structure is fairly simple: the electrons responsible for the metallic conduction and for the magnetism belong to the same double-degenerate  $e_g$  band, which is rather narrow (its width is of the

order of 1 eV) [99]. Recent band calculation of  $\text{CoS}_2$  [127] predicts a near-HMF state for this compound.

The experimental data on the magnetic properties of  $\text{Fe}_{1-x}\text{Co}_x\text{S}_2$  are reported in Ref. [100]. The most striking observation is the appearance of ferromagnetism at a very low electron concentration  $n = x < 0.05$ . This ferromagnetism is unsaturated right up to  $n \approx 0.15$  and in a wide range  $0.15 < n < 0.95$  the magnetic moment corresponds to one Bohr magneton per electron. However, in contrast to weak itinerant ferromagnets such as the Ni–Rh alloys there is no evidence of the exchange enhancement of the Pauli susceptibility in the paramagnetic range of temperatures and the Curie–Weiss law is satisfied at all electron concentrations. Moreover, the Curie constant is proportional to  $n$ . This behaviour cannot be explained by the  $t$ -matrix approximation of Kanamori [101], which is a modified variant of the Stoner theory: the ground ferromagnetic state at low values of  $n$  is obtained in this approach if there is a sharp density-of-states peak near the bottom of the band, but according to the band calculations there is no such peak [99]. Moreover, the Kanamori theory cannot explain the Curie–Weiss law.

In this section we shall consider, following Ref. [4], the problem of formation of the saturated (half-metallic) and unsaturated ferromagnetic states in a narrow energy band.

The local moments in systems with the Hubbard subbands can naturally be described, in terms of the narrow-band Hubbard model of Eqn (5.5), as singly occupied sites where holes play the role of charge carriers. A calculation of the spin Green function (dynamic magnetic susceptibility) on the basis of this model and in the presence of an external field  $h$  gives

$$\begin{aligned} G_q(\omega) &= \left[ 2\langle S^z \rangle + \sum_k \frac{(\varepsilon_{k-q} - \varepsilon_k)(n_k^+ - n_{k-q}^-)}{\omega - h - E_k^+ + E_{k-q}^-} \right] \\ &\times \left[ \omega - h - \sum_k \frac{(\varepsilon_{k-q} - \varepsilon_k)(\varepsilon_{k-q} n_{k-q}^- - \varepsilon_k n_k^+)}{\omega - h - E_k^+ + E_{k-q}^-} \right]^{-1}, \end{aligned} \quad (7.1)$$

where—according to Eqn (5.8)—we have

$$\begin{aligned} E_k^\sigma &= (n_0 + n_\sigma)\varepsilon_k = \left( \frac{1+c}{2} + \sigma\langle S^z \rangle \right) \varepsilon_k, \\ n_k^\sigma &= (n_0 + n_\sigma) f\left( E_k^\sigma + \sigma \frac{h}{2} \right). \end{aligned} \quad (7.2)$$

The magnetisation equation is obtained in a similar to the Tyablikov approach for the Heisenberg model [102]:

$$\langle S^z \rangle = \frac{1-c}{2} + \frac{1}{\pi} \int_{-\infty}^{\infty} d\omega N_B(\omega) \sum_q \text{Im} G_q(\omega). \quad (7.3)$$

Eqn (7.3) can be simplified if  $\langle S^z \rangle \ll 1$ , i.e. for the paramagnetic phase when  $\langle S^z \rangle = \chi h$ , and also when the electron concentration is low  $n = 1 - c$  at any temperature. Expansion of the numerator and denominator in Eqn (7.1) makes it possible to separate explicitly the dependence on  $\langle S^z \rangle$  and  $h$ :

$$G_q(\omega) = \frac{\omega A_q(\omega) + \langle S^z \rangle B_q(\omega) + h C_q(\omega)}{\omega - \langle S^z \rangle D_q(\omega) - h P_q(\omega)}. \quad (7.4)$$

The quantity  $A$ , which governs the value of the effective magnetic moment, is

$$A_q(\omega) = \sum_k \frac{f(E_{k-q}) - f(E_k)}{\omega + E_{k-q} - E_k} \times \left[ 1 + \frac{2}{1+c} \sum_k \frac{E_{k-q} f(E_{k-q}) - E_k f(E_k)}{\omega + E_{k-q} - E_k} \right]^{-1}, \quad (7.5)$$

$$E_k = \frac{1+c}{2} \varepsilon_k.$$

If the condition  $\langle S^z \rangle \neq 0$  is obeyed, Eqn (7.1) has a real pole, which governs the spin-wave frequency  $\omega_q$ .

If  $c \ll 1$  (almost half-filled band), then at  $T = 0$  we have  $\langle S^z \rangle = (1-c)/2$ , i.e. the ground state is a saturated ferromagnet in accordance with the Nagaoka theorem [79]. At low temperatures the Bloch law applies:

$$\langle S^z \rangle = \frac{1-c}{2} - \sum_p N_B(\omega_p), \quad (7.6)$$

$$\omega_p = \sum_k (\varepsilon_{k-p} - \varepsilon_k) f(\varepsilon_k). \quad (7.7)$$

Eqn (7.7) differs from the exact result for the spin-wave spectrum [39, 79] by corrections which are small in terms of the reciprocal coordination number  $1/z$ .

If the electron concentration is low,  $n \ll 1$ , the spin-wave frequency is

$$\omega_q = \langle S^z \rangle \sum_k \varepsilon_k \left[ \varepsilon_{k-q} \frac{f(\varepsilon_{k-q}) - f(\varepsilon_k)}{\varepsilon_{k-q} - \varepsilon_k} - \varepsilon_k \frac{\partial f(\varepsilon_k)}{\partial \varepsilon_k} \right]. \quad (7.8)$$

The structure of this expression resembles the corresponding result of the RKKY indirect exchange theory, but in contrast to this theory, Eqn (7.8) includes the spectrum  $\varepsilon_k$  in place of the interaction parameters; this substitution is typical of the narrow-band limit. The solution of this equation for the magnetisation at  $T = 0$  when  $n \ll 1$  gives

$$S_0 = \frac{n}{2} - \frac{1}{\pi} \int_{-\infty}^0 d\omega \operatorname{Im} \sum_q A_q(\omega) = \frac{\eta n}{2}, \quad (7.9)$$

$$\eta = 2 \sum_{k,q} \frac{(\varepsilon_{k-q} - \varepsilon_k) \theta(\varepsilon_{k-q} - \varepsilon_k)}{\varepsilon_{k-q} - \varepsilon_k + \varepsilon_{\max} - \varepsilon_q},$$

and the positive quantity  $\eta < 1$  is formally small in terms of  $1/z$ . In the 'Debye model' with  $\varepsilon_k = a + bk^2$  ( $k < k_D$ ) we find that  $\eta = \frac{1}{4}$ . In view of the smallness of  $\eta$ , the ferromagnetism is strongly unsaturated at low values of  $n$ .

If  $\langle S^z \rangle = \chi h(T > T_C)$  is substituted in Eqn (7.4), the following equation is obtained for the paramagnetic susceptibility  $\chi$ :

$$\frac{1-c}{2} + \frac{1}{\pi} \int_0^{\infty} d\omega \coth \frac{\omega}{2T} \operatorname{Im} \sum_q A_q(\omega) = T \sum_q \left[ \frac{\chi B_q(0) + C_q(0)}{\chi D_q(0) + P_q(0)} + A_q(0) \right]. \quad (7.10)$$

The Curie temperature is determined by the condition  $\chi^{-1}(T_C) = 0$ . If  $n \ll 1$ , its value

$$T_C = \frac{S_0}{2} \left[ \sum_q D_q^{-1}(0) \right]^{-1} = \frac{S_0}{2} \frac{\varepsilon_{\max}^2 m^* k_F}{2\pi^2} v_0 \quad (7.11)$$

is small compared with typical electron energies, so that at  $T \sim T_C$  the carriers are strongly degenerate. If  $T_C \ll T \ll E_F$ , then

$$\chi = -\frac{1}{4} \sum_k \frac{\partial f(\varepsilon_k)}{\partial \varepsilon_k} + \frac{C}{T - \theta}. \quad (7.12)$$

The Curie constant  $C$  is half the saturation magnetisation  $S_0$  (as in the case of localised spins, we have  $S = \frac{1}{2}$ ). The paramagnetic Curie temperature

$$\theta = C \sum_q D_q(0) \quad (7.13)$$

considered in the lowest order in the electron concentration is identical with  $T_C$ . If  $n$  is not too small, the dependence of  $D$  on  $q$  becomes important and a large positive difference  $\theta - T_C$  appears. Therefore, in agreement with the experimental data on  $\text{Fe}_{1-n}\text{Co}_n\text{S}_2$  the Curie-Weiss law has the Curie constant proportional to  $n$ . It should be pointed out that degeneracy of the conduction band of the  $e_g$  type does not play a major role in the range of high values of  $U$  and low values of  $n$ , but is important when  $n = 1 - c \approx 1$  (for example, this is true of the ferromagnetic metal  $\text{CoS}_2$ , which—strictly speaking—cannot be described by the theory under consideration).

If  $c \ll 1$ , we have the local moment at each site and a small number of carriers (holes). It is then found that the conditions for strong degeneracy of carriers at  $T \approx T_C$  is no longer satisfied. A calculation of the Curie temperature on the assumption that carriers are nondegenerate gives

$$T_C = |\varepsilon_{\min}| c^{1/2}. \quad (7.14)$$

The susceptibility at  $T \gg T_C$  also obeys the Curie-Weiss law.

The estimate (7.14) is valid if carriers are of their usual band nature. The possibility of their self-trapping, demonstrated in Ref. [103], may alter the results.

It follows that within the framework of the adopted approximation the ferromagnetism is stable right down to arbitrarily low electron concentrations. The concentration of holes at which the saturated ferromagnetism is destroyed is formally small in terms of  $1/z$  [39]. Numerical estimates of this hole concentration obtained by a direct variational method for square and simple cubic lattices are given in Ref. [104].

It is obvious that the fairly rough interpolation adopted here overestimates the trend to ferromagnetism at low values of  $n$  because of the neglect of fluctuations of the hole occupation numbers and because there is a critical concentration  $n_c$  at which ferromagnetism disappears. The approaches based on an expansion starting from a half-filled band may give fairly high values of this concentration (see, for example, Ref. [82]). However, the results given here provide a satisfactory description of the magnetic properties of the  $\text{Fe}_{1-x}\text{Co}_x\text{S}_2$  system.

It is interesting to compare the results reported here for narrow-band Hubbard systems with the picture of ferromagnetism used for the Kondo lattices in Refs [88, 89, 92]. A specific mean-field approximation is used there for the strong-coupling regime (at temperatures low compared with the Kondo temperature  $T_K$ ), which makes it possible to reduce the  $s$ - $f$  exchange model to an effective hybridisation model. The hybridisation parameter  $V_\sigma$  is governed by an anomalous average of the product of the operators of the conduction electrons and of the Abrikosov pseudofermions describing the subsystems [105]. An investigation of the self-consistency equations shows that for a constant 'bare' density of states there is always a solution corresponding

to a Kondo HMF state with a lower energy than a nonmagnetic state. In this state, as in the Hubbard model with strong correlations [or in the equivalent  $s-d(f)$  model with  $I \rightarrow -\infty$ ], each conduction electron compensates one localised spin, so that  $\langle S^z \rangle = (1-n)/2$ . Therefore, the similarity to a narrow-gap Hubbard ferromagnet is governed by an increase in the small ‘bare’  $s-f$  exchange parameter in the strong coupling range. An increase in the interspin Heisenberg exchange parameter is accompanied by a first-order transition to the conventional magnetic state with the fully suppressed Kondo effect ( $V_\sigma = 0$ ,  $\langle S^z \rangle = \frac{1}{2}$ ).

## 8. Microscopic model of transition-metal magnetism: analogies with half-metallic ferromagnets

Theoretical investigations of HMFs are interesting not only in the case of specific applications to compounds of the Heusler alloy type, but are also relevant to the general problem of magnetism of metals. We shall now consider the application of some of the ideas and concepts from the physics of HMFs to ‘strong’ itinerant magnetic materials, particularly Fe and Ni [6, 106].

In contrast to strongly correlated magnetic materials such as  $\text{Fe}_{1-x}\text{Co}_x\text{S}_2$  and  $\text{CrO}_2$ , for which the Hubbard splitting is large, there are no reasons to doubt that the Stoner ferromagnetism criterion is qualitatively valid in the case of itinerant magnetic materials with a fairly wide  $d$ -band (of the order of 5 eV). This criterion is  $IN(E_F) > 1$ , where  $I$  is the effective interatomic exchange parameter (possibly subject to the many-electron renormalisation). Band calculations from first principles [8] show that the Stoner parameter varies smoothly over the periodic table of elements and the variation is not too strong, whereas the values of  $N(E_F)$  may differ by tens of times for the metals at adjacent positions in this table owing to the strong dependence  $N(E)$  and different positions of  $E_F$ . In the final analysis the necessary condition for the Stoner criterion is that in a nonmagnetic state the Fermi level should coincide with a peak of  $N(E)$  (Fig. 12). Such peaks appear because of merging of the Van Hove singularities along a certain line in the  $k$  space [7, 107]. For example, in the case of bcc iron such merging occurs along the  $P-N$  line and only the  $e_g$  electrons participate in the formation of the peak [6], exactly as in the Goodenough model [108]. An analysis for Ni is reported in Ref. [109]. It follows that only a small group of the  $d$ -electron states forming the  $N(E)$  peak is responsible for ferromagnetism.

It has been proposed that electrons belonging to this group are regarded as strongly localised and can be described by the Hubbard model; the correlations of these electrons are necessarily strong because the width of the peak is small:  $\Gamma \sim 0.1$  eV. The remaining  $s$ -,  $p$ -, and  $d$ -electrons form wide bands and are weakly hybridised with the ‘magnetic’ electrons at the peak. In the ferromagnetic phase the splitting between the spin-up and spin-down peaks is  $\Delta \sim 1-2$  eV  $\gg \Gamma$ ; in contrast to the Heusler alloys, the profiles of both peaks are similar and the lower peak is completely filled. Therefore, the behaviour of ‘magnetic’ electrons is similar to those in a saturated ferromagnet, i.e. it is close to the HMF state in the usual Hubbard model with large values of  $U$  (we recall that, according to Section 4, in this situation the descriptions

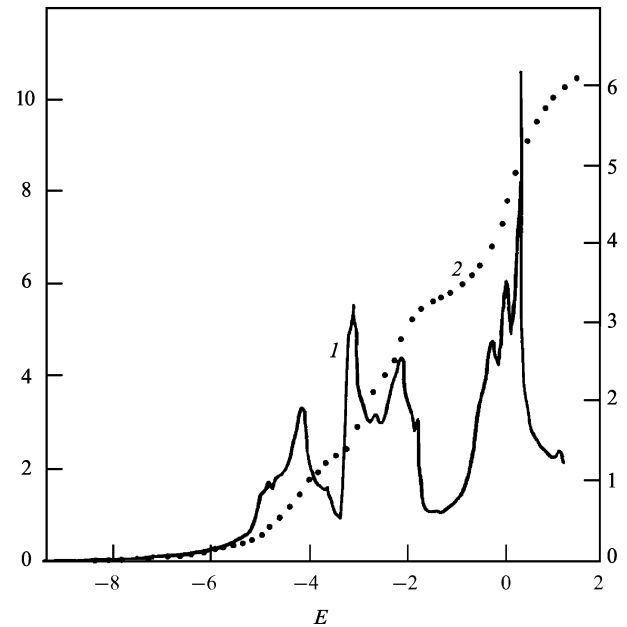


**Figure 12.** Density of states ( $\text{eV}^{-1}$ , continuous curve 1, ordinate on the right) and integral density of states (points 2, ordinate on the left) of the nonmagnetic bcc iron [8]. The energy  $E$  (eV) is measured from  $E_F$ .

based on the Hubbard splitting and on the large spin splitting are essentially equivalent). This model makes it possible to account readily for the low values (compared with the Fermi energy) of the Curie temperature, which—as demonstrated by the results in the preceding sections—should be of the order of  $T$ .

Strong (even compared with the Heusler alloys) non-quasiparticle effects can be expected in this case. These effects may be important for the explanation of the experimental data on the spin polarisation deduced from the photoemission [110] and thermionic emission [111] experiments, which are in strong conflict with the results of the band calculations of Fe and Ni. The linear term in the specific heat obtained for Ni (see Ref. [6]) is larger for the ferromagnetic phase than for the paramagnetic phase [in conflict with the Stoner theory in which the spin splitting reduces  $N(E_F)$ ], which may be related to the nonquasiparticle contributions. These contributions to the impurity resistivity, discussed above, are important in connection with the problem of the electric resistivity of ferromagnetic transition metals at very high temperatures (when contributions proportional to  $T^{3/2}$  and  $T$ , which cannot be explained by relativistic processes, are observed [2]).

We can see that comparison of the transition metals of the iron group with HMFs is at least as useful as the extrapolation from the direction of weak itinerant magnetic materials [3]. Spin-fluctuation theories make it possible only to develop a semiphenomenological theory of the temperature dependences of the magnetic and thermodynamic properties, whereas the approach under discussion provides means for investigating nontrivial problems related to the characteristics of the ground state.

## 9. Half-metallic antiferromagnets

We have seen that HMFs have properties very different from the properties of 'conventional' conducting ferromagnets. The question naturally arises as to whether these properties also apply to antiferromagnets.

The antiferromagnetic ordering splits the electron spectrum into Slater subbands [1]. In the simplest Hubbard model (or in the  $s$ - $d$  model) the electron spectrum is

$$\begin{aligned} E_k^{(1,2)} &= \theta_k \mp E_k, \quad E_k = (\tau_k^2 + U^2 \bar{S}^2)^{1/2}, \\ \bar{S} &= \sum_k \langle c_{k\uparrow}^\dagger c_{k+Q\downarrow} \rangle, \\ \theta_k &= (t_{k+(Q/2)} + t_{k-(Q/2)})/2, \\ \tau_k &= (t_{k+(Q/2)} - t_{k-(Q/2)})/2, \end{aligned} \quad (9.1)$$

where  $Q$  is the wave vector of the antiferromagnetic structure and the quantity  $\Delta = 2U\bar{S}$  represents a direct band gap. An increase in the electron-electron interaction can split the whole energy band into two, giving rise to a Slater gap. In particular, when the number of electrons becomes equal to the number of sites ( $n = 1$ ), a metal-insulator transition takes place. If the occupancy of the conduction band cannot be represented by an integer, the Fermi level crosses only one Slater subband and a system of this kind can be called a half-metallic antiferromagnet (HMAF). The case of large values of  $\Delta$  is hardly likely in intermetallic systems of the Heusler alloy type. Therefore, a more realistic situation is that in which the gap in the electron spectrum exists in the paramagnetic state and is of the hybridised origin, and the antiferromagnetic ordering shifts the Fermi level to one of the hybridised subbands, so that one of the Slater subbands is either completely empty or completely filled.

The HMAF state was predicted by the band calculations for CrMnSb with the  $C1_b$  structure [11] (see also the calculations reported in Ref. [128]). Experimental results show that this compound (as well as the  $Li_xMn_{1-n}Se$ , FeRh,  $Cr_{2-x}Mn_xSb$ , and  $Co_{2-x}Mn_xSb$  systems [112]) undergo a transition from the antiferromagnetic to the ferromagnetic phase when temperature is increased. This instability can be explained as follows [11]. In the AMnSb system the moment of the A sites is antiparallel to the moment of Mn, which results in a reduction in the band energy because of the formation of the gap, but the exchange energy increases because of the ferromagnetic superexchange. Passing from A = Ni to A = Cr reduces the total magnetic moment, since the moment of the A sites increases. The balance of these contributions in CrMnSb may induce a semiconductor-metal transition in one of the spin subbands, which is accompanied by a change in the nature of the magnetic ordering.

It is of interest to compare this situation with the behaviour of the compound UNiSn [46, 47, 113] which has the  $C1_b$  structure and in which an antiferromagnetic metal-paramagnetic semiconductor transition takes place when temperature is increased to  $T = 47$  K (this is a transition sequence opposite to the usual metal-insulator transition in the transition-metal chalcogenides [53]). This effect may also be related to 'half-metallic' features in the band structure found for a hypothetical ferromagnetic phase [18] and explained by a shift of the Fermi energy

on appearance of antiferromagnetism. An alternative possibility for the many-electron (Kondo) origin of the gap in UNiSn and its suppression by the antiferromagnetic ordering is discussed in Ref. [88].

The problem of the nature of the energy gap amounting to  $E_g \sim 10$  K in UNiSn has not yet been finally solved. The isostructural compounds ZrNiSn, TiNiSn, and HfNiSn have a large energy gap ( $E_g \sim 10^3$  K) of the band type and it is evidently associated with a 'vacancy' sublattice in their crystal structure [114] (this should be compared with the discussion of the electron spectrum of the Huesler alloys of the TMnSb type, which is given in Section 2). Any investigation of the TMSn ( $T = Ti, Zr, Hf; M = Fe, Co, Ni$ ) compounds [115] has yielded very low values of the electronic specific heat, apart from the case when  $M = Co$ . Ferromagnetism of TiCoSn with  $T_C = 143$  K has been reported and, by analogy with NiMnSb, a hypothesis has been put forward that the HMF state appears in this compound.

The compound YbNiSn has a Kondo metallic lattice in which ferromagnetic ordering with  $T_C = 5$  K and  $\mu_0 = 4\mu_B$  appears at low temperatures, and the absence of the gap is attributed to the weakness of the  $d$ - $f$  hybridisation in ytterbium compounds [116]. In the nonmagnetic Kondo insulator lattice of CeNiSn the gap is very small ( $E_g \sim 3$  K) [114]. (It is interesting to note that static spin correlations with local moments of the order of  $10^{-3}\mu_B$  are observed at ultralow temperatures in CeNiSn [117]; measurements of the longitudinal nuclear relaxation rate [118] give  $1/T_1 \propto T^2$ , which may indicate a nonzero density of nonquasiparticle states in the gap.) The evolution of the electronic properties of the  $Ce_{1-x}La_xNiSn$  [114] and  $U_{1-x}Th_xNiSn$  [113] systems with increase in  $x$  is qualitatively similar. The temperature dependences of the magnetic susceptibility [113] and of the nuclear relaxation rate [119] in UNiSn indicate that localised moments or at least strong spin fluctuations exist in this compound. All these results tend to support the Kondo origin of the gap in UNiSn.

In contrast to ferromagnets, the processes of decay of magnons with small momenta in Stoner excitations are not forbidden in antiferromagnets and one-magnon processes are effective right down to the lowest temperatures because spin-flip transitions occur within the Slater subbands. This has the effect that both in 'conventional' itinerant and in half-metallic antiferromagnets the damping of magnons is linear in  $q$  and the spin-wave contribution to the electric resistivity is proportional to  $T^5$ , as in the case of the scattering by phonons. (At temperatures  $T$  which are not too low, the contribution of the interband transitions is a quadratic function of  $T$ .) The distinguishing features of HMAFs may be deduced only from those physical properties in which the contribution of the interband transitions occurs and which have a threshold in terms of  $q$  for any conducting antiferromagnet (or ferromagnet), but are absent (at least up to energies of the order of the gap) in the half-metallic case. If  $\Delta$  is small, the interband contribution to the integral thermodynamic characteristics (for example, the thermal expansion, elastic moduli, magnetoelectric effect) is generally more singular than the contribution of the intraband transitions so that the corresponding anomalies of HMAFs should be weaker [120].

Let us consider the dynamic susceptibility of a conducting antiferromagnet. In the local coordinate system we



have

$$S_q^+ = \sum_k d_{k\uparrow}^+ d_{k+q\downarrow}, \quad S_q^z = \frac{1}{2} \sum_k (d_{k\uparrow}^+ d_{k+q\uparrow} - d_{k\downarrow}^+ d_{k+q\downarrow}),$$

$$d_{k\sigma}^+ = \frac{1}{\sqrt{2}} [c_{k+(Q/2)\uparrow}^+ + \sigma c_{k-(Q/2)\downarrow}^+]. \quad (9.2)$$

If we adopt the simplest approximation of free quasiparticles with the spectrum of Eqn (9.1) (more complex approximations, allowing for the spin-wave contributions, are not of great interest because they do not apply specifically to HMAFs; the nonquasiparticle effects in conducting antiferromagnets are discussed in Ref. [121]), we find that

$$\langle\langle S_q^+ | S_{-q}^- \rangle\rangle_\omega = \frac{1}{4} \sum_k \left[ \left(1 - \frac{\Delta}{E_k}\right) \left(1 + \frac{\Delta}{E_{k+q}}\right) \right. \\ \times \left( \frac{n_k^{(1)} - n_{k+q}^{(1)}}{\omega + E_k^{(1)} - E_{k+q}^{(1)}} + \frac{n_{k+q}^{(2)} - n_k^{(2)}}{\omega + E_{k+q}^{(2)} - E_k^{(2)}} \right) \\ + \left(1 + \frac{\Delta}{E_k}\right) \left(1 + \frac{\Delta}{E_{k+q}}\right) \frac{n_k^{(1)} - n_{k+q}^{(2)}}{\omega + E_k^{(1)} - E_{k+q}^{(2)}} \\ \left. + \left(1 - \frac{\Delta}{E_k}\right) \left(1 - \frac{\Delta}{E_{k+q}}\right) \frac{n_k^{(2)} - n_{k+q}^{(1)}}{\omega + E_k^{(2)} - E_{k+q}^{(1)}} \right], \quad (9.3)$$

$$\langle\langle S_q^z | S_{-q}^z \rangle\rangle_\omega = \frac{1}{8} \sum_k \left[ \left(1 - \frac{\tau_k \tau_{k+q} - \Delta^2}{E_k E_{k+q}}\right) \right. \\ \times \sum_{i=1,2} \frac{n_k^{(i)} - n_{k+q}^{(i)}}{\omega + E_k^{(i)} - E_{k+q}^{(i)}} + \left(1 + \frac{\tau_k \tau_{k+q} - \Delta^2}{E_k E_{k+q}}\right) \\ \left. \times \sum_{i \neq j} \frac{n_k^{(i)} - n_{k+q}^{(j)}}{\omega + E_k^{(i)} - E_{k+q}^{(j)}} \right]. \quad (9.4)$$

We can see that the contribution of the intraband transitions to the transverse susceptibility disappears (i.e. it vanishes in the case of HMAFs) only for  $\Delta \rightarrow \infty$ . If  $\Delta$  is small, the longitudinal susceptibility of HMAFs is low for  $q \rightarrow \mathbf{0}$  and large for  $q \sim Q$ . The difference from the case of ferromagnets is due to the fact that the gap appears in the electron spectrum of an antiferromagnet [Eqn (9.1)] in a more complex manner.

## 10. Conclusions

In this review we have tried to demonstrate that the study of HMFs, which started only ten years ago, has already enriched our ideas of the magnetism of metals and alloys, and much more can be expected from future specific investigations.

The theoretically most interesting is the feasibility of detecting the pure non-quasiparticle (spin-polaron) effects in HMFs. There are not many cases in the physics of the solid state when the standard Fermi liquid description is known to be insufficient. The only example of such a situation is probably the case of one-dimensional systems which are described by the Luttinger liquid model [122]. The case of two-dimensional (and, even more so, three-dimensional) systems with strong Hubbard correlations is still the subject of lively discussions [123], which are particularly topical in

connection with the problem of high-temperature superconductors. In this situation an important point is that HMFs represent a simple and convincing example of the failure of the universal validity of the theory of the Fermi liquid in the case of three-dimensional systems. From the point of view of the experimental investigations the data on the spin polarisation of charge carriers are particularly interesting; such investigations should definitely be continued. Another sensitive instrument for the study of non-quasiparticle effects is nuclear magnetic relaxation.

As pointed out above, nonquasiparticle contributions can also be observed in ‘conventional’ strong itinerant magnetic materials. In this sense the HMFs, characterised by strong intra-atomic correlations (for example, those involving the Mn ions in the Heusler alloys), by well-defined local moments, and sometimes also by a strong Hubbard splitting (true, for example, of CrO<sub>2</sub>), complement well the weak itinerant magnetic materials such as ZrZn<sub>2</sub>, which have served as the prototype of ferromagnetic metals right up to the early eighties [3].

As far as practical applications of HMFs are concerned, we have already mentioned their possible use in magneto-optic data retrieval and also in the development of new magnetic materials with a high saturation magnetisation and high Curie points. We shall mention here one other attractive possibility. The interest in magnetic multilayers, associated with the giant magnetoresistance effect [125], has grown greatly in recent years. This effect becomes stronger as the ratio of the partial static conductivity with different spin projections deviates further from unity. By the very definition of HMFs this ratio has a record value for these ferromagnets. Therefore, these materials may be promising for the fabrication of multilayers. At present, attempts have been made to form multilayers from the PtMnSb/CuMnSb system [126].

**Acknowledgements.** We are grateful to S V Vonsovskii for his interest and encouragement. The work was partly financed by the Russian Fund for Fundamental Research (grant No. 93-02-16802).

## References

1. Herring C in *Magnetism* (Eds G T Rado, H Suhl) Vol. 4 (New York: Academic Press, 1966) p. 1
2. Vonsovskii S V *Magnetism* (New York: Halsted, 1975)
3. Moriya R *Spinovye Fluktuatsii v Magnetikakh s Kollektivizirovannymi Elektronami* (Spin Fluctuations in Itinerant Electron Magnetics) (Berlin: Springer, 1985)
4. Auslender M I, Irkhin V Yu, Katsnelson M I *J. Phys. C* **21** 5521 (1988); *Fiz. Met. Metalloved.* **65** 57 (1988)
5. Dzyaloshinskii I E, Kondratenko P S *Zh. Eksp. Teor. Fiz.* **70** 1987 (1976) [*Sov. Phys. JETP* **43** 1036 (1976)]
6. Irkin V Yu, Katsnelson M I, Trefilov A V *J. Phys. Condens. Matter* **5** 8763 (1993)
7. Vonsovskii S V, Katsnelson M I, Trefilov A V *Fiz. Met. Metalloved.* **76** (3) 3 (1993)
8. Moruzzi V L, Janak J F, Williams A R *Calculated Electronic Properties of Metals* (Oxford: Pergamon Press, 1978)
9. de Groot R A, Mueller F M, van Engen P G, Buschow K H J *Phys. Rev. Lett.* **50** 2024 (1983)
10. de Groot R A, Mueller F M, van Engen P G, Buschow K H J *J. Appl. Phys.* **55** 2151 (1984)
11. de Groot R A, Buschow K H J *J. Magn. Magn. Mater.* **54–57** 1377 (1986)
12. Kubler J *Physica B+ C* **127** 257 (1984)

13. de Groot R A, von der Kraan A M, Buschow K H J *J. Magn. Magn. Mater.* **61** 330 (1986)
14. Kubler J, Williams A R, Sommers C B *Phys. Rev. B* **28** 1745 (1983)
15. Fujii S, Sugimura S, Ishida S, Asano S *J. Phys. Condens. Matter* **2** 8583 (1990)
16. Schwarz K *J. Phys. F* **16** L211 (1986)
17. Kulatov E, Mazin I *J. Phys. Condens. Matter* **2** 343 (1992); Nikolaev A V, Andreev B V *Fiz. Tverd. Tela (St Petersburg)* **35** 1185 (1993) [*Phys. Solid State* **35** 603 (1993)]
18. Albers R C, Boring A M, Daalderop G H O, Mueller F M *Phys. Rev. B* **36** 3661 (1987)
19. Kulatov E T, Khalilov S V *Zh. Eksp. Teor. Fiz.* **98** 1778 (1990) [*Sov. Phys. JETP* **71** 998 (1990)]; Halilov S V, Kulatov E T *J. Phys. Condens. Matter* **3** 6363 (1991)
20. Yanase A, Satoro K *J. Phys. Soc. Jpn.* **53** 312 (1984)
21. Wijngaard J H, Haas C, de Groot R A *Phys. Rev. B* **40** 9318 (1989)
22. van Engen P G, Buschow K H J, Jongebreur R, Erman M *Appl. Phys. Lett.* **42** 202 (1983)
23. Schwarz K, Mohn O, Blaha P, Kubler J *J. Phys. F* **14** 2659 (1984)
24. Jaswal S S *Phys. Rev. B* **41** 9697 (1990)
25. Jaswal S S, Yelon W B, Hadjipanayis G C, et al. *Phys. Rev. Lett.* **67** 644 (1991)
26. Min B I, Kang J-S, Hong J H, et al. *Phys. Rev. B* **48** 6217 (1993)
27. Malik S K, Arlinghaus F J, Wallace W E *Phys. Rev. B* **16** 1242 (1977)
28. Malik S K, Arlinghaus F J, Wallace W E *Phys. Rev. B* **25** 6488 (1982)
29. Inoue J, Shimizu M *J. Phys. F* **15** 1511 (1985)
30. Matar S, Mohn P, Demazeau G, Siberchicot B *J. Phys. (Paris)* **49** 1761 (1988)
31. Tgawa Y, Motizuki K *J. Phys. Condens. Matter* **3** 1753 (1991)
32. Fujii S, Ishida S, Asano S *J. Phys. Condens. Matter* **4** 1575 (1992)
33. Sakuma A *J. Phys. Soc. Jpn.* **60** 2007 (1990)
34. Matar S, Moohn P, Demazeau G, Schwarz K *J. Magn. Magn. Mater.* **101** 251 (1991)
35. Matar S, Mohn P, Kubler J *J. Magn. Magn. Mater.* **104–107** 1927 (1992)
36. Auslender M I, Irkhin V Yu, Katsnelson M I *J. Phys. C* **17** 669 (1984)
37. Auslender M I, Irkhin V Yu *J. Phys. C* **18** 3533 (1985)
38. Irkhin V Yu, Katsnel'son M I *Zh. Eksp. Teor. Fiz.* **88** 522 (1985) [*Sov. Phys. JETP* **61** 306 (1985)]
39. Irkhin V Yu, Katsnelson M I *J. Phys. C* **18** 4173 (1985)
40. Irkhin V Yu, Katsnelson M I *J. Phys. Condens. Matter* **2** 7151 (1990)
41. Irkhin V Yu, Katsnel'son M I *Fiz. Tverd. Tela (Leningrad)* **25** 3383 (1983) [*Sov. Phys. Solid State* **25** 1947 (1983)]
42. de Groot R A, van Engen P G, van Engelen P P J, Buschow K H J *J. Magn. Magn. Mater.* **86** 326 (1990)
43. Brandle H, Weller D, Parkin S S P, et al. *Phys. Rev. B* **46** 13889 (1992)
44. Argyres P N *Phys. Rev.* **97** 334 (1955)
45. van Engen P G, Buschow K H J, Erman M *J. Magn. Magn. Mater.* **30** 374 91983)
46. Kawanaka H, Fujii H, Nishi M, Takabatake T, et al. *J. Phys. Soc. Jpn.* **58** 3481 (1989)
47. Yethiraj M, Robinson R A, Rhyne J J, Gotaas J A, Buschow K H J *J. Magn. Magn. Mater.* **79** 355 (1989)
48. Weller D, Reim W, Ebert H, Johnson D D, Pinski F J *J. Phys. (Paris)* **49** Colloq. 8 C8–41 (1988)
49. van der Heide P A M, Baelde W, de Groot R A, et al. *J. Phys. F* **15** L75 91985)
50. Brandle H, Weller D, Scott J C, et al. *Proceedings of International Conference on Physics of Transition Metals, Darmstadt, 1992 in Int. J. Modn. Phys. B* **7** 345 (1993)
51. Kisker E, Carbone C, Flipse C F, Wassermann E F *J. Magn. Magn. Mater.* **70** 21 (1987)
52. Kamper K P, Schmitt W, Guntherodt G, Gambino R J, Ruf R *Phys. Rev. Lett.* **59** 2788 (1987)
53. Mott N F *Metal–Insulator Transitions* (London: Taylor and Francis, 1974)
54. Chase L L *Phys. Rev. B* **10** 2226 (1974)
55. Mori H *Prog. Theor. Phys.* **34** 339 (1965)
56. Irkhin Yu P, Voloshinskii A N, Abelskii Sh Sh *Phys. Status Solidi* **22** 309 (1967)
57. Otto M J, Feil H, van Woerden R A M, et al. *J. Magn. Magn. Mater.* **70** 33 (1987)
58. Otto M J, Feil H, van Woerden R A M, van der Valk P J, et al. *J. Phys. Condens. Matter* **1** 2351 (1989)
59. Bona G L, Meier F, Taborelli M, Bucher E, Schmidt P H *Solid State Commun.* **56** 391 (1985)
60. Webster P J *J. Phys. Chem. Solids* **32** 1221 (1971)
61. Ido H *J. Magn. Magn. Mater.* **54–57** 937 (1986)
62. Ido H, Yasuda S *J. Phys. (Paris)* **49** Colloq. 8 C8–141 (1988)
63. Otto M J, van Woerden R A M, van der Valk P J, et al. *J. Phys. Condens. Matter* **1** 2341 (1989)
64. Gyorffy B L, Pindor A J, Staunton J, Stocks G M, Winter H *J. Phys. F* **15** 1337 (1985)
65. Turzhevskii S A, Likhtenshtein A I, Katsnel'son M I *Fiz. Tverd. Tela (Leningrad)* **32** 1952 (1990) [*Sov. Phys. Solid State* **32** 1138 (1990)]
66. Ooiwa K, Endo K, Shinogi A *J. Magn. Magn. Mater.* **104–107** 2011 (1992)
67. Noda Y, Ishikawa Y *J. Phys. Soc. Jpn.* **40** 690, 699 (1976)
68. Tajima K, Ishikawa Y, Webster P J, et al. *J. Phys. Soc. Jpn.* **43** 483 (1977)
69. Moriya T *J. Phys. Soc. Jpn.* **19** 681 (1964)
70. Turov E A, Petrov M P *Nuclear Magnetic Resonance in Ferro- and Antiferromagnets* (New York: Wiley, 1972)
71. Enokiya H *J. Phys. Soc. Jpn.* **31** 1037 (1971)
72. Matsuura M *J. Phys. Soc. Jpn.* **21** 886 (1966)
73. Mizoguchi T, Inoue M *J. Phys. Soc. Jpn.* **21** 310 (1966)
74. Ikhin V Yu, Entelis A M *Phys. Status Solidi B* **169** 189 (1992)
75. Izyumov Yu A, Kassan-Ogly F A, Skryabin Yu N *Polevye Metody v Teori Ferromagnetizma* (Field Methods in the Theory of Ferromagnetism) (Moscow: Nauka, 1974)
76. Methfessel S, Mattis D C in *Handbuch der Physik* (Ed. H P J Wijn) Vol. 18, Part I (Berlin: Springer, 1968) pp 389–562
77. Hertz J A, Edwards D M *J. Phys. F* **3** 2174 (1973); Edwards D M, Hertz J A *J. Phys. F* **3** 2191 (1973)
78. Hubbard J *Proc. R. Soc. London Ser. A* **276** 238 (1963)
79. Nagaoka Y *Phys. Rev.* **147** 392 (1966)
80. Vonsovskii S V, Katsnel'son M I *Usp. Fiz. Nauk* **158** 723 (1989) [*Sov. Phys. Usp.* **32** 720 (1989)]
81. Anderson P W in *Proceedings of Summer School on "Frontiers and Borderlines in Many-Particle Physics"*, Varenna, 1987 (Amsterdam: North-Holland, 1988) p.000
82. Vedyayev A V, Nikolaev M Yu *Pis'ma Zh. Eksp. Teor. Fiz.* **41** 18 (1985) [*JETP Lett.* **41** 20 (1985)]; Nikolaev M Yu, Ryzhanova N V, Vedyayev A V, Zubritskii S M *Phys. Status Solidi B* **128** 513 (1985)
83. Edwards D M *J. Phys. C* **16** L327 (1983)
84. Auslender M I, Irkhin V Yu *Solid State Commun.* **50** 1003 (1984)
85. Kisker E, Baum G, Mahan H, Raith W, Reihl B *Phys. Rev. B* **18** 2256 (1978)
86. Auslender M I, Irkhin V Yu *Z. Phys. B* **56** 301 (1984); **61** 129 (1985)
87. Irkhin V Yu, Katsnelson M I *Z. Phys. B* **75** 67 (1989)
88. Irkhin V Yu, Katsnelson M I *Z. Phys. B* **82** 77 (1991)
89. Irkhin V Yu, Katsnelson M I *Fiz. Met. Metalloved.* (1) 16 (1991); *J. Phys. Condens. Matter* **2** 8715 (1990)
90. Irkhin V Yu, Katsnelson M I *J. Phys. Condens. Matter* **4** 9661 (1992)
91. Silin V P, Solontsov A Z *Fiz. Met. Metalloved.* **58** 1080 (1984)
92. Irkhin V Yu, Katsnelson M I *Fiz. Met. Metalloved.* **71** (1) 16 (1991)
93. Abrikosov A A, Dzyaloshinskii I E *Zh. Eksp. Teor. Fiz.* **35** 771 (1958) [*Sov. Phys. JETP* **8** 535 (1959)]

94. Abrikosov A A, Gor'kov L P, Dzyaloshinskii I E *Methods of Quantum Field Theory in Statistical Physics* (Englewood Cliffs, NJ: Prentice-Hall, 1963)
95. Carneiro G M, Pethick C J *Phys. Rev. B* **11** 1106 (1975)
96. Vollhardt D *Rev. Mod. Phys.* **56** 99 (1984)
97. Fraga G L F, Brandao D E, Sereni J G *J. Magn. Magn. Mater.* **102** 199 (1991)
98. Irkhin V Yu, Katsnelson M I, Trefilov A V *Physica C (Utrecht)* **160** 397 (1989)
99. Lauer S, Trautwein A X, Harris F E *Phys. Rev. B* **29** 6774 (1984)
100. Jarrett H S, Cloud W H, Bouchard R J, et al. *Phys. Rev. Lett.* **21** 617 (1968)
101. Kanamori J *Prog. Theor. Phys.* **30** 275 (1963)
102. Tyablikov S V *Methods in the Quantum Theory of Magnetism* (New York: Plenum, 1967)
103. Brinkman W F, Rice T M *Phys. Rev. B* **2** 1324 (1970)
104. von der Linden W, Edwards D M *J. Phys. Condens. Matter* **3** 4917 (1991)
105. Coleman P, Andrei N *J. Phys. Condens. Matter* **1** 4057 (1989)
106. Irkhin V Yu, Katsnel'son M I, Trefilov A V *Pis'ma Zh. Eksp. Teor. Fiz.* **53** 351 (1991) [*JETP Lett.* **53** 367 (1991)]; *J. Magn. Magn. Mater.* **117** 210 (1992)
107. Katsnel'son M I, Peschanskikh G V, Trefilov A V *Fiz. Tverd. Tela (Leningrad)* **32** 470 (1990) [*Sov. Phys. Solid State* **32** 272 (1990)]
108. Goodenough J B *Phys. Rev.* **120** 67 (1960)
109. Daalderop G H O, Boon M H, Mueller F M *Phys. Rev. B* **41** 9803 (1990)
110. Chrobok G, Hofmann M, Regenfus G, Sizmann R *Phys. Rev. B* **15** 429 (1977)
111. Vaterlaus A, Milani F, Meier F *Phys. Rev. Lett.* **65** 3041 (1990)
112. Goodenough J B *Magnetism and the Chemical Bond* (New York: Interscience, 1963)
113. Fujii H, Kawanaka H, Takabatake T, et al. *J. Magn. Magn. Mater.* **87** 235 (1990)
114. Aliev F G, Brandt N B, Kozyrkov V V, et al. *Pis'ma Zh. Eksp. Teor. Fiz.* **45** 535 (1987) [*JETP Lett.* **45** 684 (1987)]; Aliev F G, Moshchalkov V V, Kozyrkov V V, et al. *J. Magn. Magn. Mater.* **76–77** 295 (1988)
115. Kuentzler R, Claud R, Schmerber G, Dossman Y *J. Magn. Magn. Mater.* **104–107** 1976 (1992)
116. Kasaya M, Tani T, Kawate K, et al. *J. Phys. Soc. Jpn.* **60** 3145 (1991)
117. Kyogaku M, Kitaoka Y, Asayama K, Takabatake T, Fujii K *J. Phys. Soc. Jpn.* **61** 43 (1992)
118. Kyogaku M, Kitaoka Y, Nakamura H, et al. *J. Phys. Soc. Jpn.* **59** 1728 (1990)
119. Kojima K, Hukuda Y, Kawanaka H, et al. *J. Magn. Magn. Mater.* **90–91** 505 (1990)
120. Irkhin V Yu, Katsnel'son M I, Trefilov A V *Pis'ma Zh. Eksp. Teor. Fiz.* **56** 317 (1992) [*JETP Lett.* **56** 315 (1992)]
121. Irkhin V Yu, Katsnelson M I *J. Phys. Condens. Matter* **3** 6439 (1991)
122. Mahan G D *Many-Particle Physics* (New York: Plenum, 1981)
123. Anderson P W *Phys. Rev. Lett.* **64** 1839 (1990); **65** 2306 (1990); **66** 3226 (1991); **71** 1220 (1993)
124. Katsnelson M I, Edwards D M *J. Phys. Condens. Matter* **4** 3289 (1992)
125. *Proceedings of First International Symposium on Magnetic Multilayers, Kyoto, 1993* in *J. Magn. Magn. Mater.* **126** (1993)
126. Takanashi K, Watanabe M, Fujimori H *J. Appl. Phys.* **67** 393 (1990)
127. Zhao G L, Callaway J, Hayashibara M *Phys. Rev. B* **48** 15781 (1993)
128. Wijngaard J H, Haas C, de Groot R A *Phys. Rev. B* **45** 5395 (1992)